PHYS 7363 - Experimental Particle Detection and Detectors I

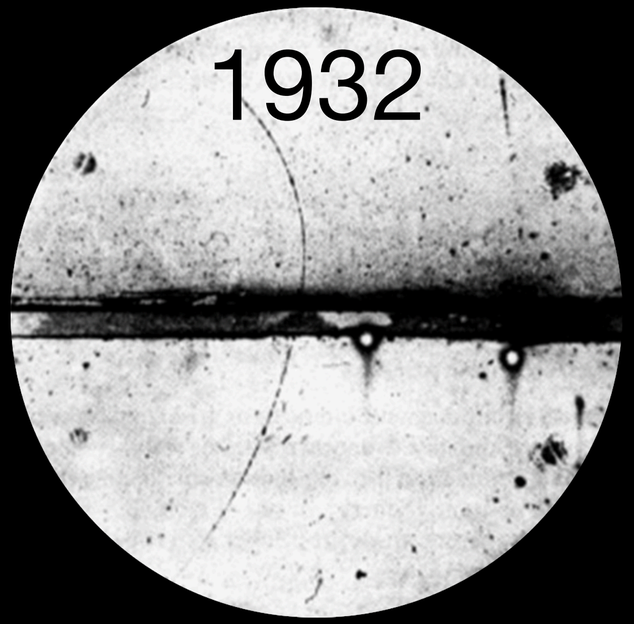

2017

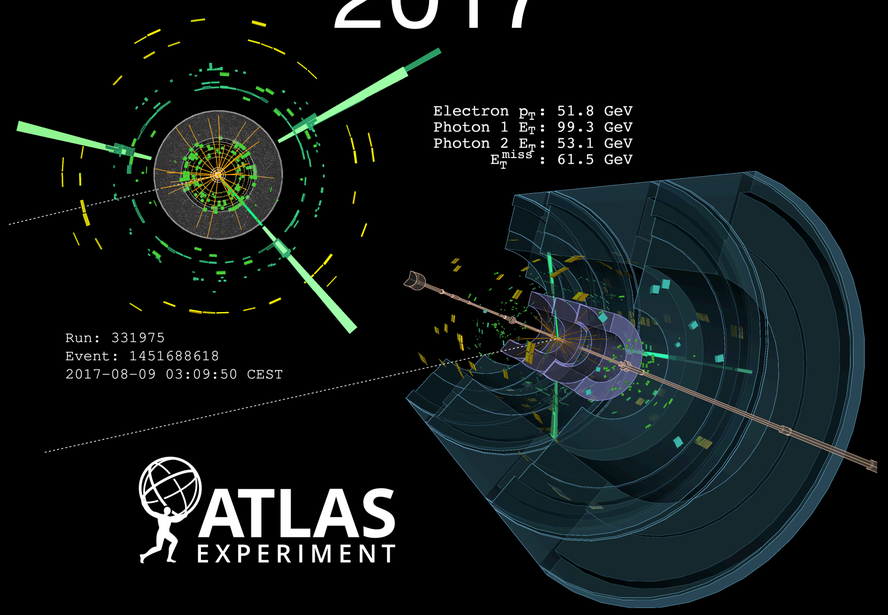

Particle detectors are the workhorses of experimental physics. In this course, we'll dive deep into their physics, exploring the incredible evolution of our experimental techniques over the past nine decades. You'll gain a solid understanding of *particle detection* and *identification*, examine the intricate designs of modern detectors, and learn how machine learning is being harnessed to push the boundaries of detector design. If you're intrigued by how we “see” subatomic particles, this course is for you!

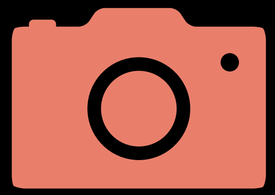

Detect

Identify

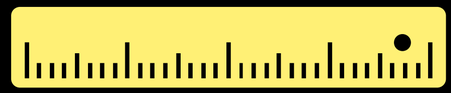

Measure

To discuss prerequisites (and any questions on the content of the course), please contact me: saptaparnab@smu.edu

Schedule

Month	Monday	Tuesday	Wednesday	Thursday	Friday	Saturday	Sunday
August	18	19	20	21	22	23	24
	25 ✅	26	27	28	29 ✅	30	31
September	1	2	3 ✅	4	5 ✅	6	7
	8 1.5 hours	9	10	11	12	13	14
	15 ✅ 1.5 hours	16	17 1.5 hours	18	19 1.5 hours	20	21
	22 1.5 hours	23	24 1.5 hours	25	26 1.5 hours	27	28
October	29 1.5 hours	30	1 1.5 hours	2	3 1.5 hours	4	5

Schedule

Month	Monday	Tuesday	Wednesday	Thursday	Friday	Saturday	Sunday
October	6	7	8	9	10	11	12
	13	14	15	16	17	18	19
	20	21	22	23	24	25	26
	27	28	29	30	31	1	2
November	3	4	5	6	7	8	9
	10	11	12	13	14	15	16
	17	18	19	20	21	22	23
	24	25	26	27	28	29	30
December	1	2	3	4	5	6	7
	8	9	10	11	12	13	14

Key dates

- Weeks 1-4: Particle interaction with matter
  - Interaction of charged and neutral particles
  - Particle showers
- Weeks 5-9: Detector technologies:
  - Tracking detectors (gaseous detectors, semiconductor detectors)
  - Particle detection with photons (scintillators, Cherenkov detectors)
  - Calorimetry (electromagnetic and hadronic calorimeters)
- Weeks 10-12: Large and small scale experiments:
  - Triggering and data acquisition
  - Tracking
  - Full reconstruction (particle flow)
- Week 13-15: Preparation for final project:
  - FCC-ee: https://indico.fnal.gov/event/67484/contributions/314057/attachments/187076/257915/US%20FCC%20Tutorial_FullSim.pdf
  - Muon collider: https://mcd-wiki.web.cern.ch/software/tutorials/fermilab2024/

Resources

- PDG review: Passage of particles through matter
  - https://pdg.lbl.gov/2020/reviews/rpp2020-rev-passage-particles-matter.pdf
- N. Wermes / H. Kolanoski, “Particle Detectors”, Oxford University Press, 2020
- Georg Viehhauser/Tony Weinberg, “Detectors in Particle Physics: A Modern Introduction”, CRC Press, Taylor and Francis Group
- C. Grupen / B. Schwartz, “Particle Detectors”, Cambridge University Press, 2011
- F. Hartmann, “Evolution of Silicon Sensor Technology in Particle Physics”
- A. Strandlie, R. Frühwirth, Pattern Recognition, Tracking and Vertex Reconstruction in Particle Detectors
- LHC experiment design: https://www.nature.com/articles/nature06078

Particle interaction with matter

Particle detection through interaction

- Particles can be detected by their interaction with matter. Detectors typically use the following processes:
  - Ionization and excitation of atoms in media by charged particles (electron-ion pairs)
  - bremsstrahlung: photon radiation emitted by charged particles in the fields of atomic nuclei
  - photon scattering (Compton scattering) and photon absorption (registers the presence of light by absorbing photons and converting that absorbed energy into an electrical signal, such as a current or voltage, proportional to the number of photons)
  - Cherenkov (charged particle traveling faster than speed of light in a medium) and transition radiation
  - nuclear reactions: hadrons (p, n, π, α) with nuclear matter
  - weak interactions constituting the only possibility to detect neutrinos

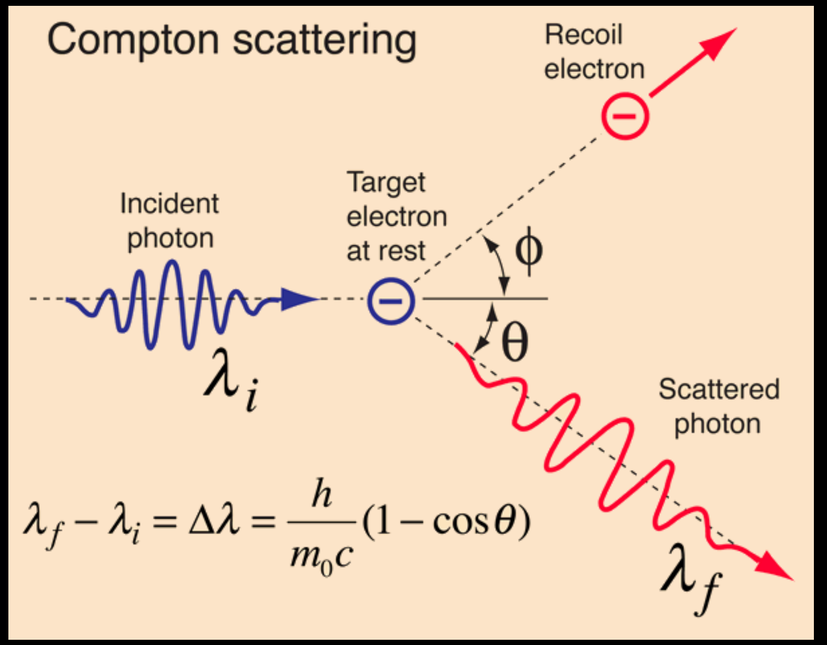

Energy loss of charged particles by ionization

- Consider projectile with mass M ($M \gg m_e$), charge ze and 4-momentum vectors: P and P' before and after the interaction
- The 4-momentum vectors: p_e and p'_e before and after the interaction
- With the 4-momentum transfer:
  - $Q^2 = -(P - P')^2 = -(p - p'_e)^2$
  - Lorentz-invariant form of Rutherford scattering:
    - $$\frac{d\sigma}{dQ^2} = \frac{4\pi z^2 \alpha^2 \hbar^2 c^2}{\beta^2} \frac{1}{Q^2}$$
    - Here βc is the velocity of the particles relative to each other
    - In the system in which the on-shell electron is at rest, it has an energy $E_e = m_e c^2$ before the collision

Bethe-Bloch formula

$$-\left\langle \frac{dE}{dX} \right\rangle = K\frac{Z}{A}\rho\frac{z^2}{\beta^2}\left[\frac{1}{2}\ln\left(\frac{2m_e c^2\beta^2\gamma^2 T_{\max}}{I^2}\right) - \beta^2 - \frac{\delta(\beta\gamma)}{2} - \frac{C(\beta\gamma, I)}{Z}\right]$$

$K = 4\pi N_A r_e^2 m_e c^2 = 0.307$ MeV cm^2/mol, using the classical electron radius

z, β: charge and velocity of the projectile

Z, A are the atomic number and mass

I is the mean excitation energy

$T_{\max}$ is the maximum possible energy transfer to a shell electron

δ is the density correction, important at high energies

C/Z is a shell correction (one has to take into account that the atomic electrons of the material traversed are not stationary)

Mean energy loss of charge particles by ionization

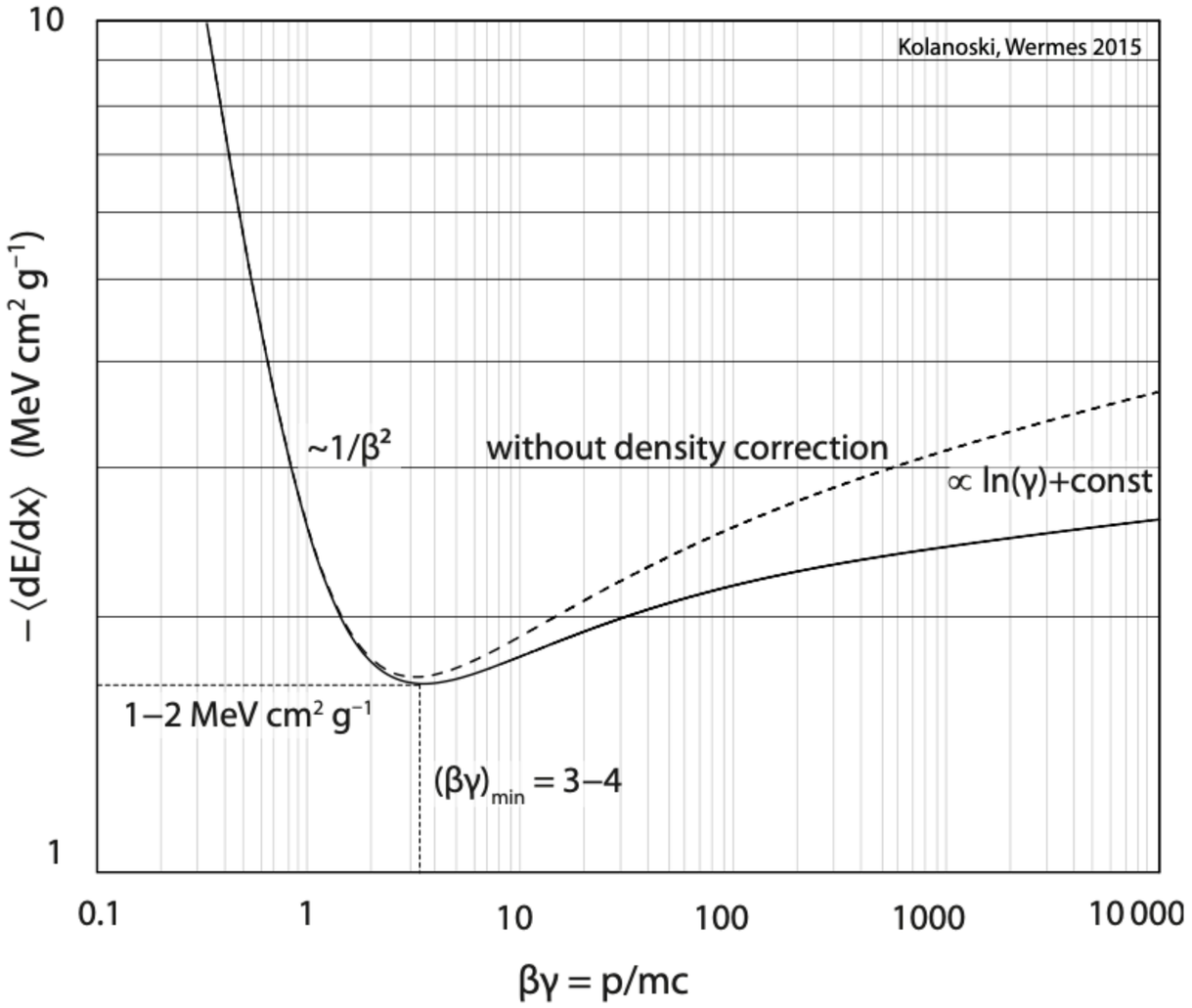

Fig. 3.5 Mean energy loss of charged particles by ionisation as a function of $\beta\gamma = p/mc$, here given for charged pions in silicon. The range indicated for the minimum of the energy loss is valid for most media. At high energies the density effect is evident as the deviation from the log γ trend due to the polarisation of the medium by the charged particle and hence screening further extension of the transverse electric field.

The Bethe–Bloch formula describes how particles are stopped in matter

Understanding the distribution

- The mean energy loss $-\left\langle \frac{dE}{dX} \right\rangle$ as a function of the energy of the in- coming particle for a typical example (π in silicon).
- At low energies the $1/\beta^2$ term dominates
- At high energies the $\ln \gamma$ term is dominant
- In between both regions there is a broad minimum around $\beta\gamma \approx 3 – 3.5$ ($\beta \approx 0.95$) depending on Z.
- Particles in this kinematic range are thus called *minimum-ionising particles* (*mips*).
- Since the increase in $\frac{dE}{dX}$ for energies corresponding to βγ > 3.5 is only moderate compared to the steep rise $\propto 1/\beta^2$ towards energies lower than the minimum, it is common practice to use the term *mip* for all charged particles with energies larger than those at the minimum

Understanding the distribution

- Low energy regime:
  - The $1/\beta^2$ dependence can be explained by the fact that the momentum transfer increases with the effective interaction time Δt which is longer for slower particles
- High energy regime:
  - Asymptotic increase of the maximum energy transfer T_{max} with γ: purely kinematic effect
  - For subtlety of large impact parameter and increasing transverse extension of the electric field with γ refer to the book!

Statistical fluctuations of energy loss

- Energy loss process has a statistical nature exhibiting fluctuations
- The energy loss ΔE along a distance Δx is composed on many small contributions δE_n corresponding to individual ionization or excitation process:
  - $$\Delta E = \sum_{n=1}^{N} \delta E_n$$
  - Statistical fluctuations occur for the number N of ionization/excitation processes but also for the emitted energy δE in these processes
  - Both produce fluctuations in the energy lost by a particle and also in the energy deposited in a material thickness Δx
  - These are commonly called *Landau fluctuations*

Number fluctuations

- In thin detectors, as often used to measure track so charged particles, poison statistic us revelant for the number of ionizations N
- The resolution on ΔE by a measurement of the number of e^--ion pairs can be estimated using Poisson statistics
  - $$\frac{\sigma(\Delta E)}{\Delta E} \approx \frac{1}{\sqrt{N}}$$

Poisson Statistics

- Poisson distribution with the expectation λ events in a given interval, the probability of κ events in the same interval is:
  - $$\frac{\lambda^k e^{-\lambda}}{\kappa!}$$
- “For instance, consider a call center which receives an average of $\lambda = 3$ calls per minute at all times of day. If the number of calls received in any two given disjoint time intervals is independent, then the number κ of calls received during any minute has a Poisson probability distribution. Receiving $\kappa = 1$ to 4 calls then has a probability of about 0.77, while receiving 0 or at least 5 calls has a probability of about 0.23.”

https://en.wikipedia.org/wiki/Poisson_distribution

Energy transfer fluctuations

- An important contribution to the total energy loss fluctuations originates from fluctuations in the amount δE of energy transferred in an individual process
- Influence on measurements:
  - Momentum resolution of a charge particle is deteriorated if the particle loses energy before or during the momentum measurement
  - For particle identification by measuring $\left\langle \frac{dE}{dx} \right\rangle$, the resolution to separate particle species depends substantially on the width of the $\left\langle \frac{dE}{dx} \right\rangle$ distribution
  - Tracking detectors suffer a reduction in space resolution by the statistical fluctuations of the ionization clusters along a track

What do read from the book

- Landau-Vavilov distribution:
  - The energy loss ΔE over a fixed distance Δx follows a probability density $f(\Delta E; \Delta x)$, which is normalized in an interval between minimal and maximal energy transfer:
  - $$\int_{\Delta E_{min}}^{\Delta E_{max}} f(\Delta E; \Delta x) d\Delta E = 1$$
  - The individual contributions of δE_n to ΔE are statistically independent, the *central limit theorem* of statistics states that ΔE is normally distributed for $N \to \infty$

Suppression of fluctuations

- Strong fluctuations of the energy loss limit the resolution on energy-momentum measurements
- Fluctuations can be reduced if the most probable value (maximum of the Landau distribution) can be used as an energy loss estimator
- Resolution can be improved by suppressing fluctuations:
  - (a) If δ-electrons can be detected and be excluded from the measurement
  - (b) largest or smallest values in a series of measurements are discarded from the calculation of the mean (truncated mean)
  - (c) if the very large energy deposits along a particle track can be measured and used for correction of the energy loss

Practical implementation

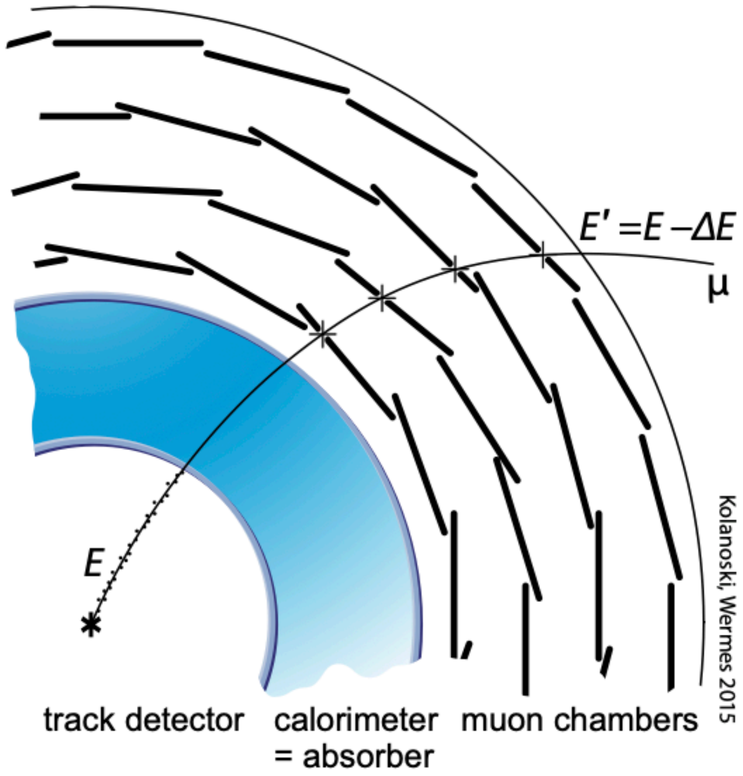

Fig. 3.15 Measurement of muon momenta in a collider detector. The sketch assumes the same magnetic field in the inner and outer tracking detectors. The energy loss, in particular in the massive calorimeter, leads to a more and more increasing curvature of the track.

- To optimally reconstruct particle tracks for a precise momentum measurement, one usually corrects for the energy loss along a particle's flight path
- To do this, one must take the average dE/dx lost over some distance of this path
- Momentum measurement can be improved if one is able to measure the actual energy loss (e.g to δ rays)

Practical implementation

- An example of such a procedure is the reconstruction of muons in the ATLAS experiment at the LHC
- The muon’s momentum can be measured stand-alone in the outer air toroid region of the detector in a large volume with magnetic field and little material
- Before reaching the muon spectrometer, the muons traverse the inner tracking detector and the calorimeter
- The largest amount of energy is lost in the calorimeters including 17 cm of lead and 125 cm of iron in the central region

What to read

- Range: energy loss by ionization the range R of a charge particle in matter has a specific value with only a small dispersion
- Because of the $1/\beta^2$ shape of the Bethe-Bloch curve at low energies, at the end of the particle's path, much energy is lost over a relatively small distance. This enhancement in deposited energy is called the Bragg peak

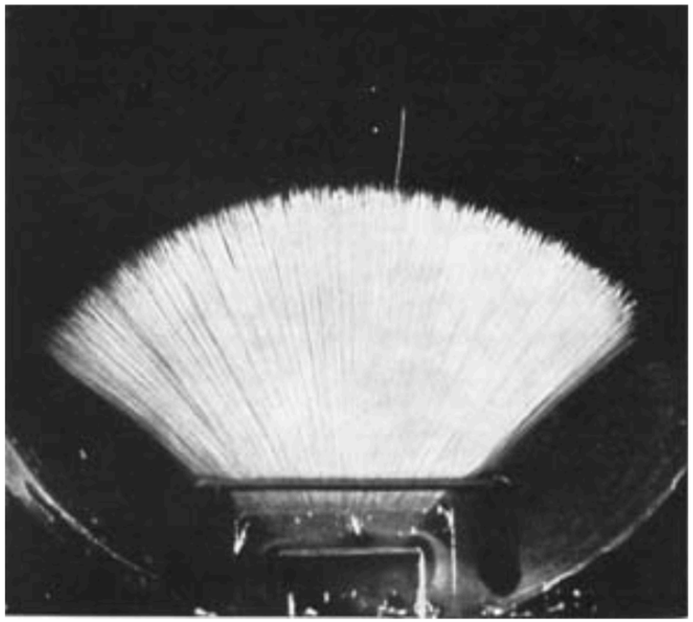

Fig. 3.21 Tracks of α particles from a radioactive decay appearing in a cloud chamber (adapted from [410], reprinted with kind permission by Springer Science+Business Media, see also [781]). The range of the particles has a sharp cut-off, which means that all α particles have the same energy. There is one track with a longer range originating from an excited nuclear state.

Checklist: Particle detection through interaction

- Particles can be detected by their interaction with matter. Detectors typically use the following processes:
  - Ionization and excitation of atoms in media by charged particles (electron-ion pairs): ✅
  - bremsstrahlung: photon radiation emitted by charged particles in the fields of atomic nuclei ✅
  - photon scattering (Compton scattering) and photon absorption (registers the presence of light by absorbing photons and converting that absorbed energy into an electrical signal, such as a current or voltage, proportional to the number of photons)
  - Cherenkov (charged particle traveling faster than speed of light in a medium) and transition radiation
  - nuclear reactions: hadrons (p, n, π, α) with nuclear matter
  - weak interactions constituting the only possibility to detect neutrinos

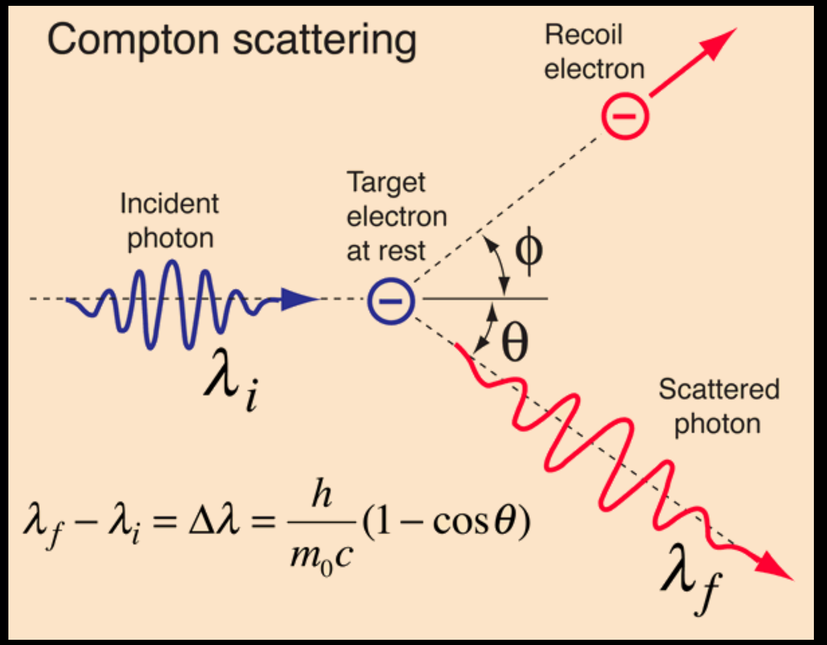

Energy loss through bremsstrahlung

- We have treated energy loss of charge particle when penetrating matter as caused by their interaction with atomic shell (excitation and ionization)
- Charged particles can also lose energy by radiating electromagnetic quanta
- Radiation from accelerated charges:
  - In classical electrodynamics, the energy emitted per unit time from an accelerated charge is computed as:
    - $$\frac{dW}{dt} = \frac{2}{3}\frac{z^2e^2}{4\pi\epsilon_0 c^3}|\ddot{\vec{x}}|^2 \propto \frac{z^4Z^2e^6}{m^2}$$
    - considering a particle with charge ze at a fixed distance r being decelerated by the field of the nucleus with charge Ze ($m\ddot{x} = zZe^2/r$)

Energy loss through bremsstrahlung

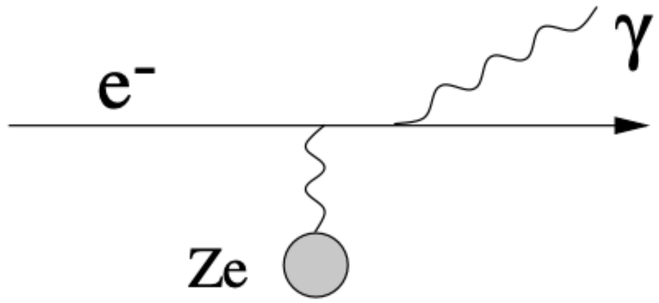

Fig. 3.23 Bremsstrahlung due to the interaction of a charged particle with the Coulomb field of a nucleus.

- The energy loss is inversely proportional to the squared mass of the decelerated particle
- A computation employing relativistic quantum electrodynamics yields a proportionality of Z^2E/m^2 of the radiated power
- The Z^2 dependence if characteristic for coherent scattering processes off a nucleus, in contrast to ionization
- Assume bremsstrahlung of electrons/positron with relativistic energies ($E \gg mc^2$)

What to read

- Energy spectrum of bremsstrahlung
  - Charge screening of the nucleus
  - Coulomb correction
  - Dielectric suppression
  - Scattering off shell electrons
  - LMP effect
- Angular distribution of bremsstrahlung

Radiation length

- Averaging the radiated energies over the bremsstrahlung spectrum yields the mean energy loss per path length:
  - $\frac{dE}{dx} = \frac{N_A \rho}{A} \int_0^E E_\gamma \frac{d\sigma}{dE_\gamma} dE_\gamma$
  - $\frac{dE}{dx} = 4\alpha r_e^2 \frac{N_A \rho}{A} E \left[(Z^2 (L_{rad} - f(Z)) + Z L'_{rad}) + \frac{1}{18}(Z^2 + Z) \right]$
  - $L_{rad}(Z)$ and $L'_{rad}(Z)$: radiator functions
  - $\left(\frac{dE}{dx} \right)_{rad} = -\frac{E}{X_0}$
  - $E(x) = E_0 e^{-\frac{x}{X_0}}$
  - After a path length $x = X_0$, an electron on average possesses only $1/e$ of its initial energy
  - The fraction $1 - 1/e \approx 63\,\%$ has been radiated off

What to read

- Radiation length
- Critical energy

Energy loss of high energy muons

- The energy loss by bremsstrahlung scales with the inverse squared mass of the radiating particle: $\frac{1}{m^2}$
- Energy loss:
  - Sum of loss from ionization and bremsstrahlung
  - $-\frac{dE}{dx} = a(E) + b(E)E$
- Ionization loss: $a(E)$
- Bremsstrahlung: $b(E)E$

Energy loss of high energy muons

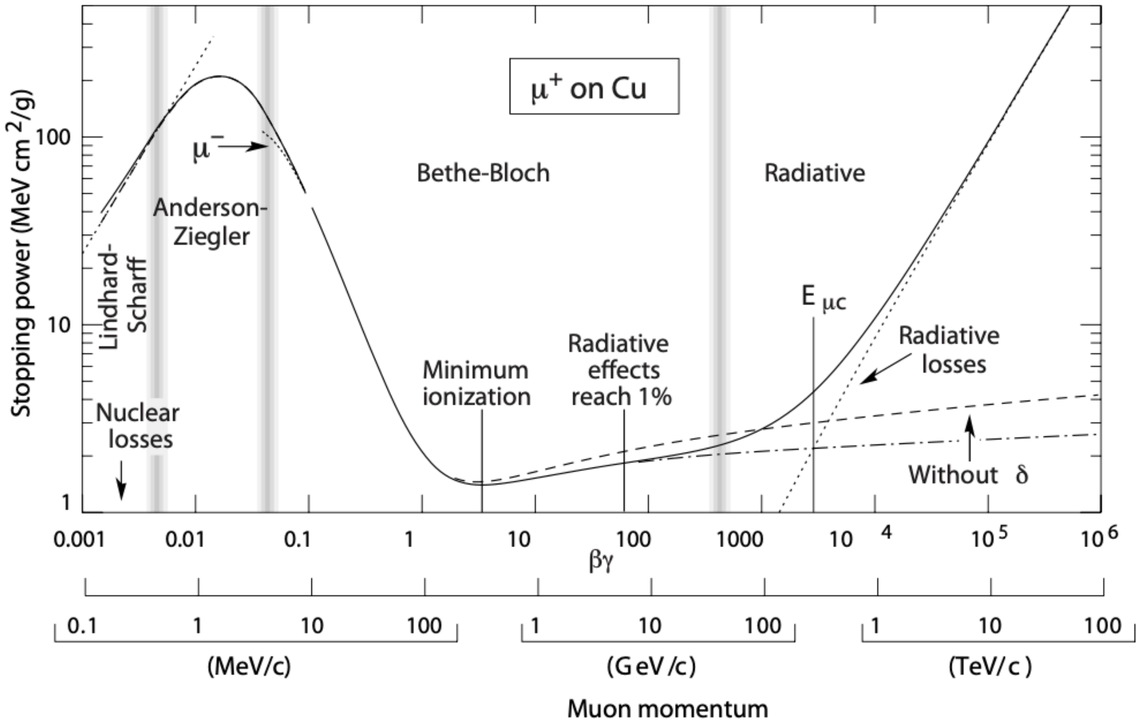

Fig. 3.28 Energy loss for positive muons in copper (taken from [746]; see also detailed description and references therein). The vertical bands separate regions with different theoretical descriptions. The centre marks the validity region of the Bethe–Bloch formula (3.25). At high energies where bremsstrahlung dominates the drawn curves show the total energy loss (solid), the loss by radiation (dotted) as well as by ionisation without (dashed) and with (dash-dotted) the inclusion of the δ term in (3.25). The region at low energies labelled 'Anderson–Ziegler' is described by an empirical fit to measured data. The region below this, labelled 'Lindhard–Scharff', is based on a theoretical model which yields an energy loss dependence roughly proportional to β (dashed line). At the lowest energies non-ionising energy loss caused by elastic nuclear recoil dominates. At low energies the energy loss is smaller for negative than for positive particles ('Barkas effect' [153]) attributed to higher order corrections and indicated here by the curve labelled μ^-.

are given in table 3.4.

Energy loss of high energy muons

- Read ahead:
  - Multiple Coulomb scattering…

Final project

Key dates

- Weeks 1-4: Particle interaction with matter
  - Interaction of charged and neutral particles
  - Particle showers
- Weeks 5-9: Detector technologies:
  - Tracking detectors (gaseous detectors, semiconductor detectors)
  - Particle detection with photons (scintillators, Cherenkov detectors)
  - Calorimetry (electromagnetic and hadronic calorimeters)
- Weeks 10-12: Large and small scale experiments:
  - Triggering and data acquisition
  - Tracking
  - Full reconstruction (particle flow)
- Week 13-15: Preparation for final project:
  - FCC-ee: https://indico.fnal.gov/event/67484/contributions/314057/attachments/187076/257915/US%20FCC%20Tutorial_FullSim.pdf
  - Muon collider: https://mcd-wiki.web.cern.ch/software/tutorials/fermilab2024/

Using Graph Neural Networks for HGCAL reconstruction

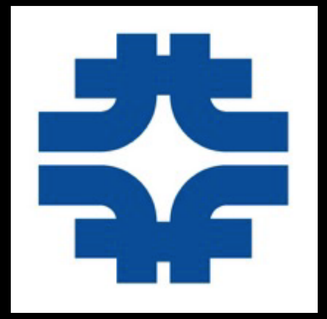


Saptaparna Bhattacharya, Matteo Cremonesi, Daniel Gaytán-Villarreal, Lindsey Gray, Jan Kieseler

2024 CMS ML Town Hall, September 30th, 2024

The power of new detectors

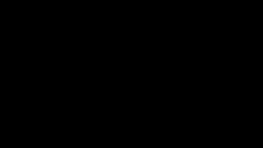

<u>Location of the High Granularity Calorimeter HGCAL:</u>

- $1.5 < \eta < 3.0$

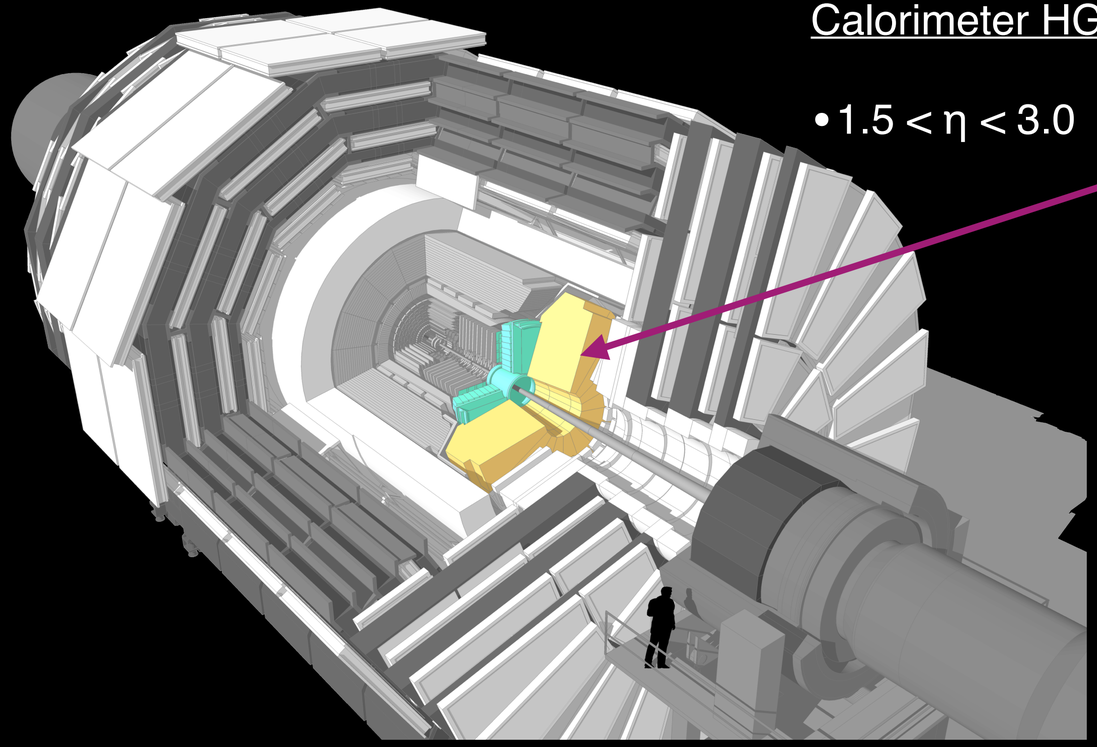

- DAQ system designed to cope with the large amount of space-energy-time information in the HL-LHC conditions
- Considerable R&D for software and computing needs and development of efficient algorithms for reconstruction

- Endcap Timing Layer
- HGCAL Thermal Screen
- Polyethelene Moderator

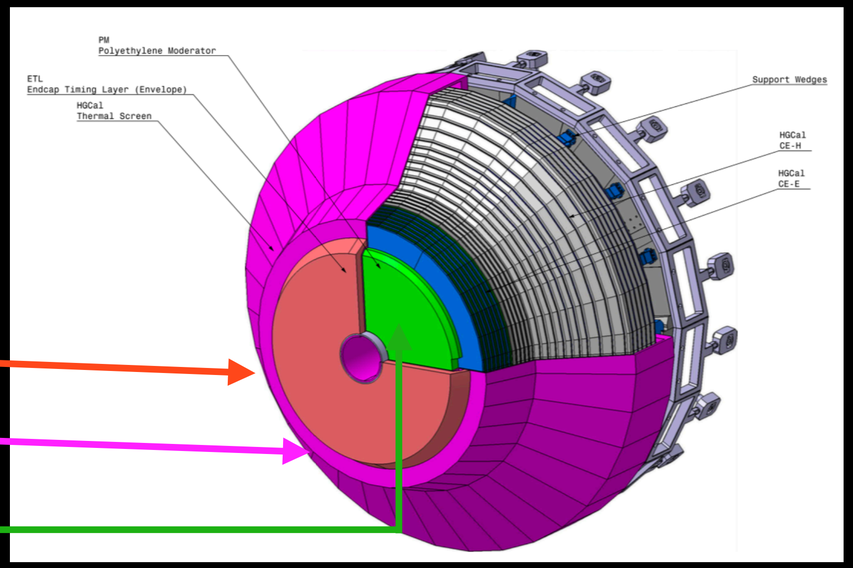

Lots of sensors: can collect a number of inputs

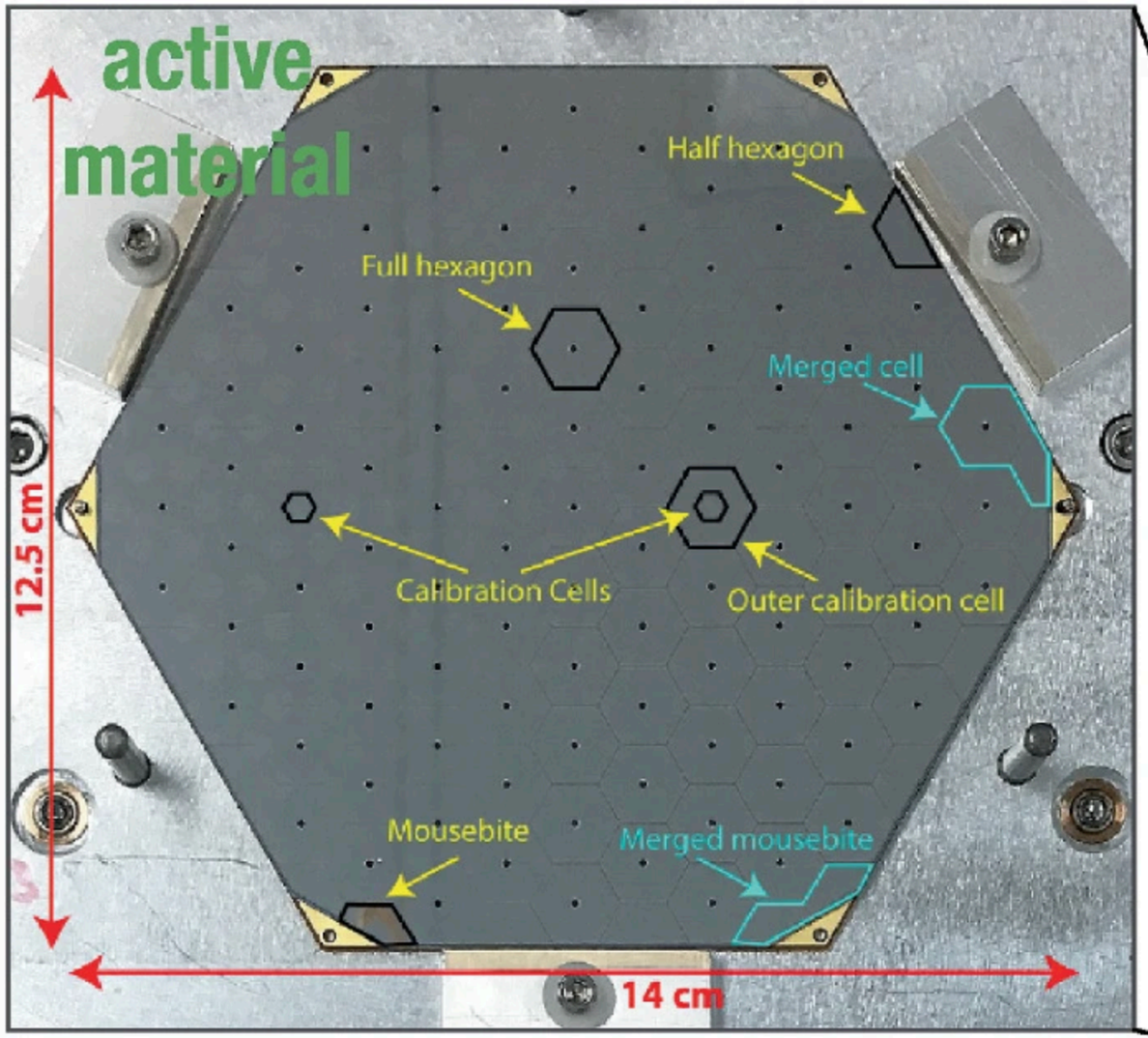

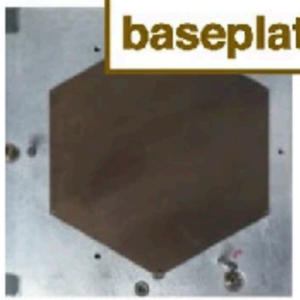

- CuW
- Cu

- Gold plated

+

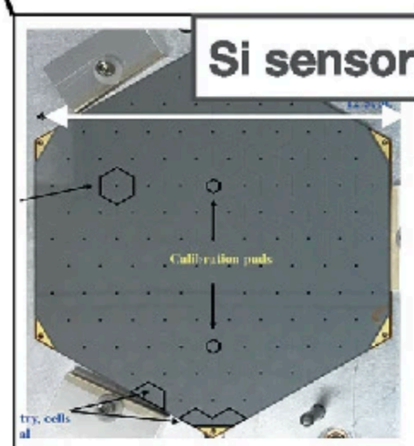

6" silicon sensors:

- n-type, 128 cells
- 1 cm² cell-size
- depletion: 200 & 300μm

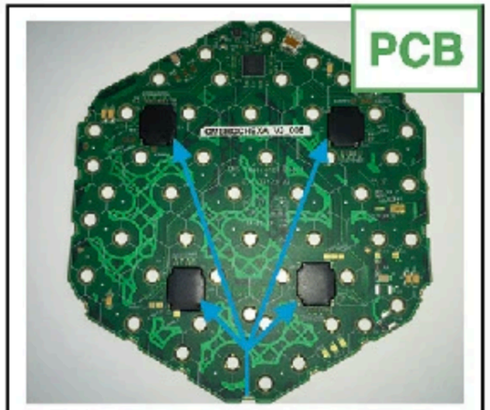

- **SKIROC2-CMS** ASIC, 64 ch., 4 chips/module
- Developed for CALICE (Skiroc2) & adjusted for HGCAL requirements

What the detector “sees”

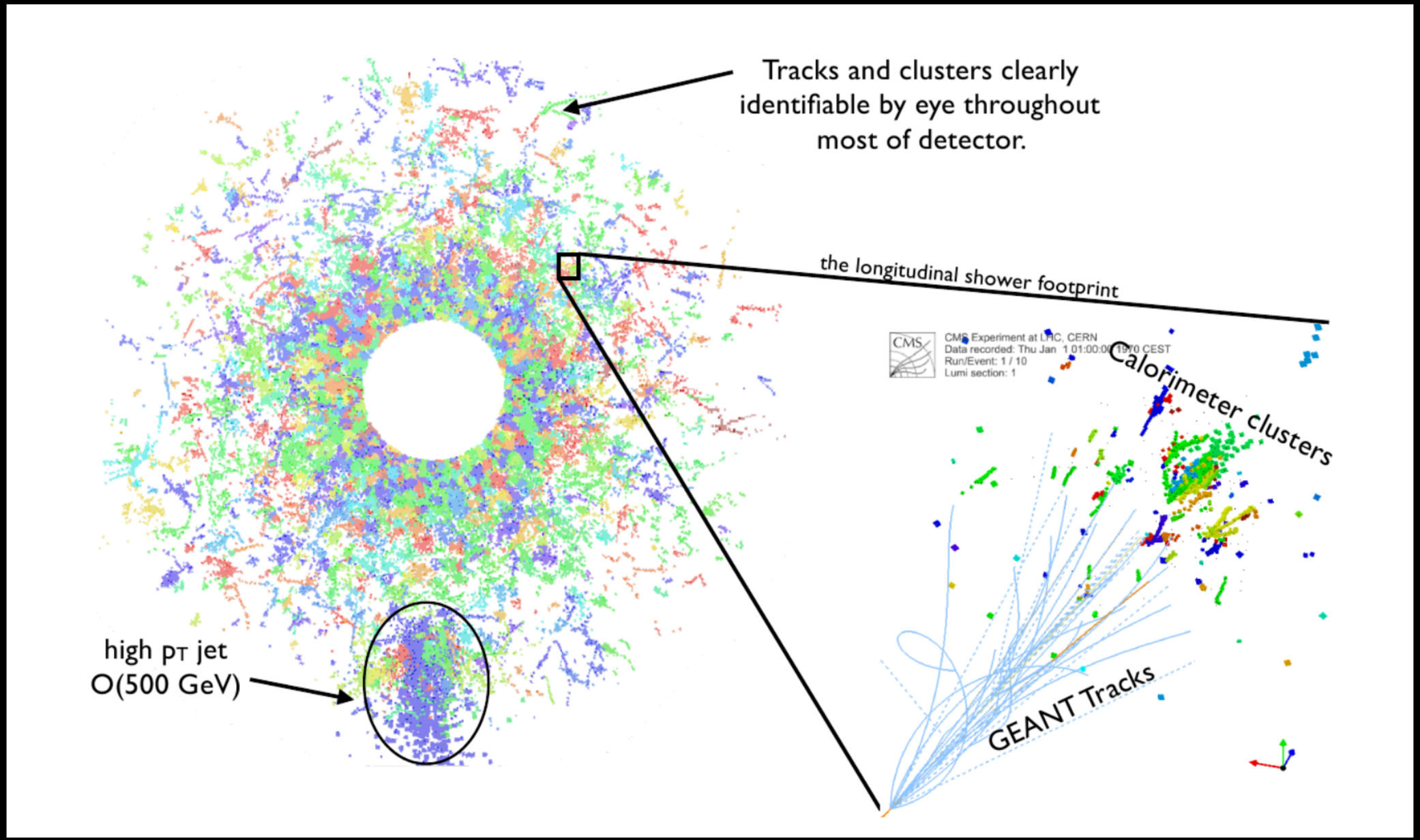

Electromagnetic showers in the detector

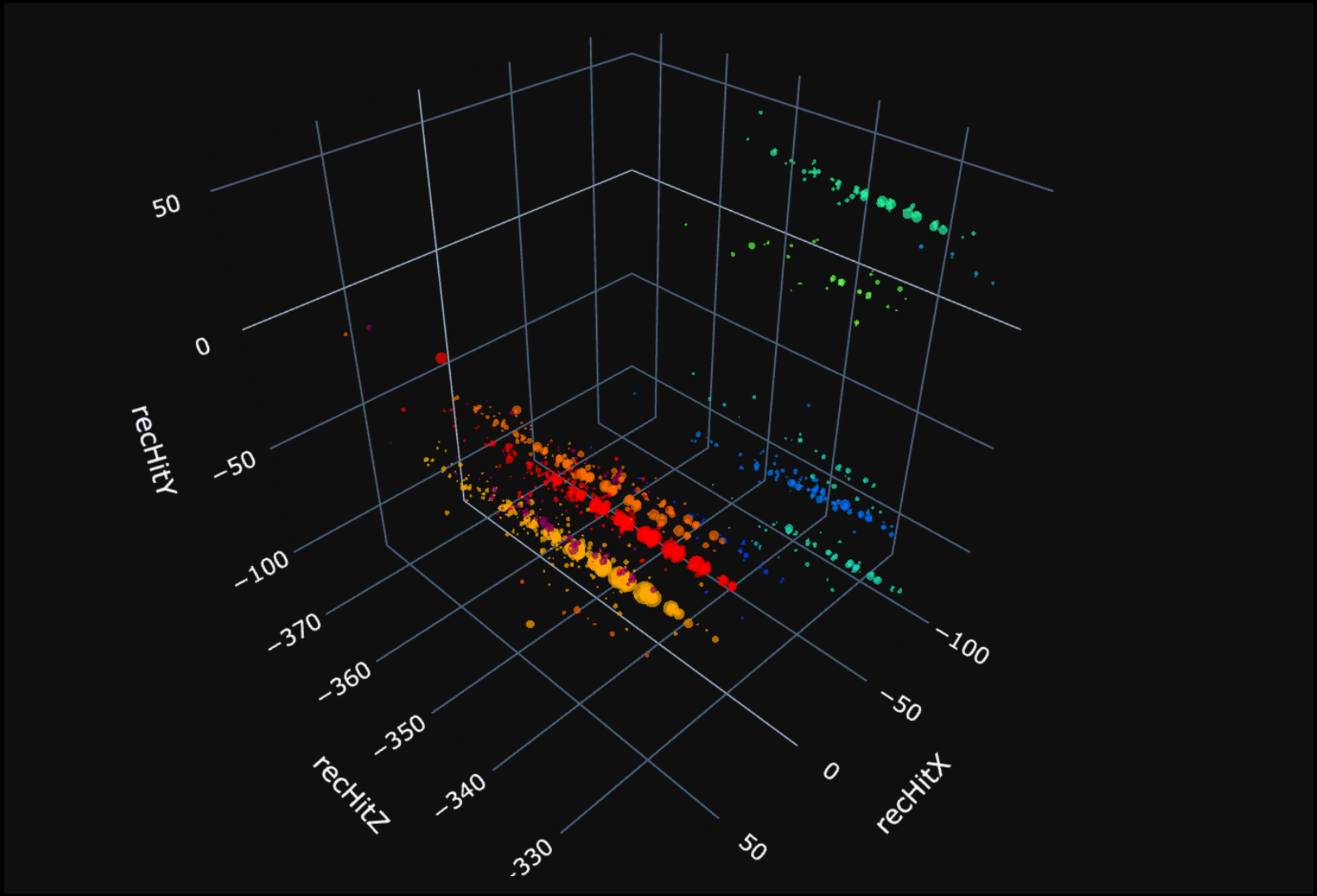

Hadronic showers in the detector

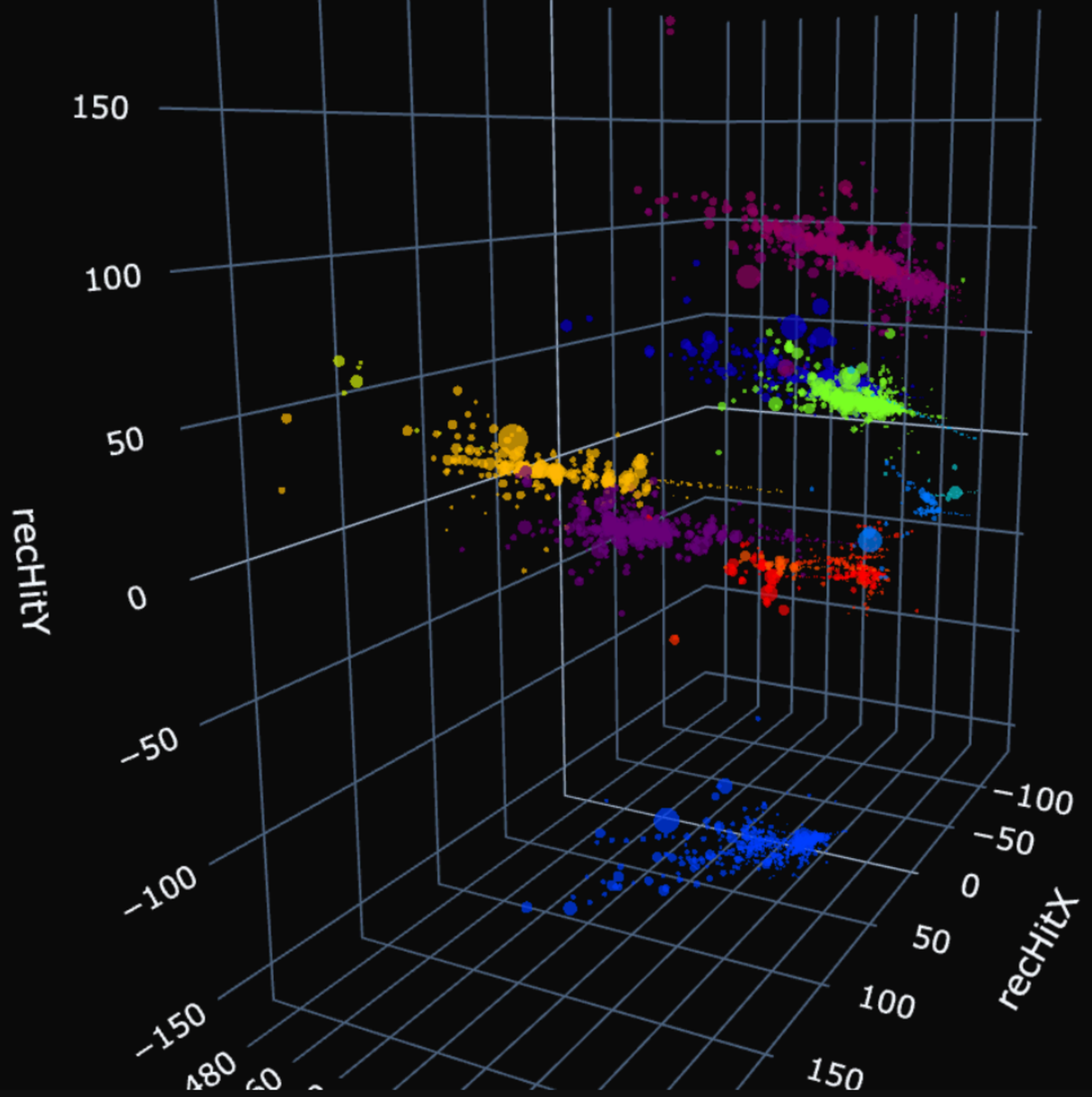

ML for HGCAL

- Unprecedented spatial granularity
- 3D visualization of showers
- Use graph neural networks!

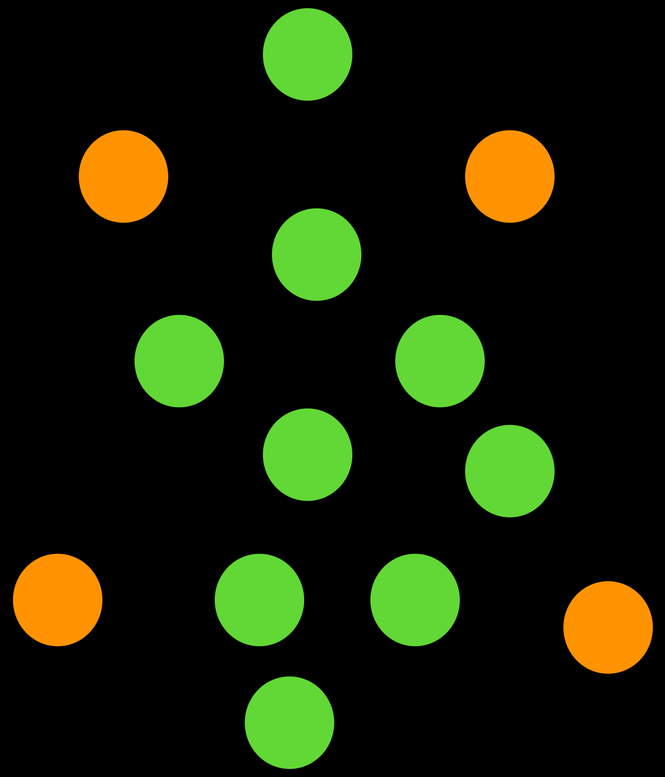

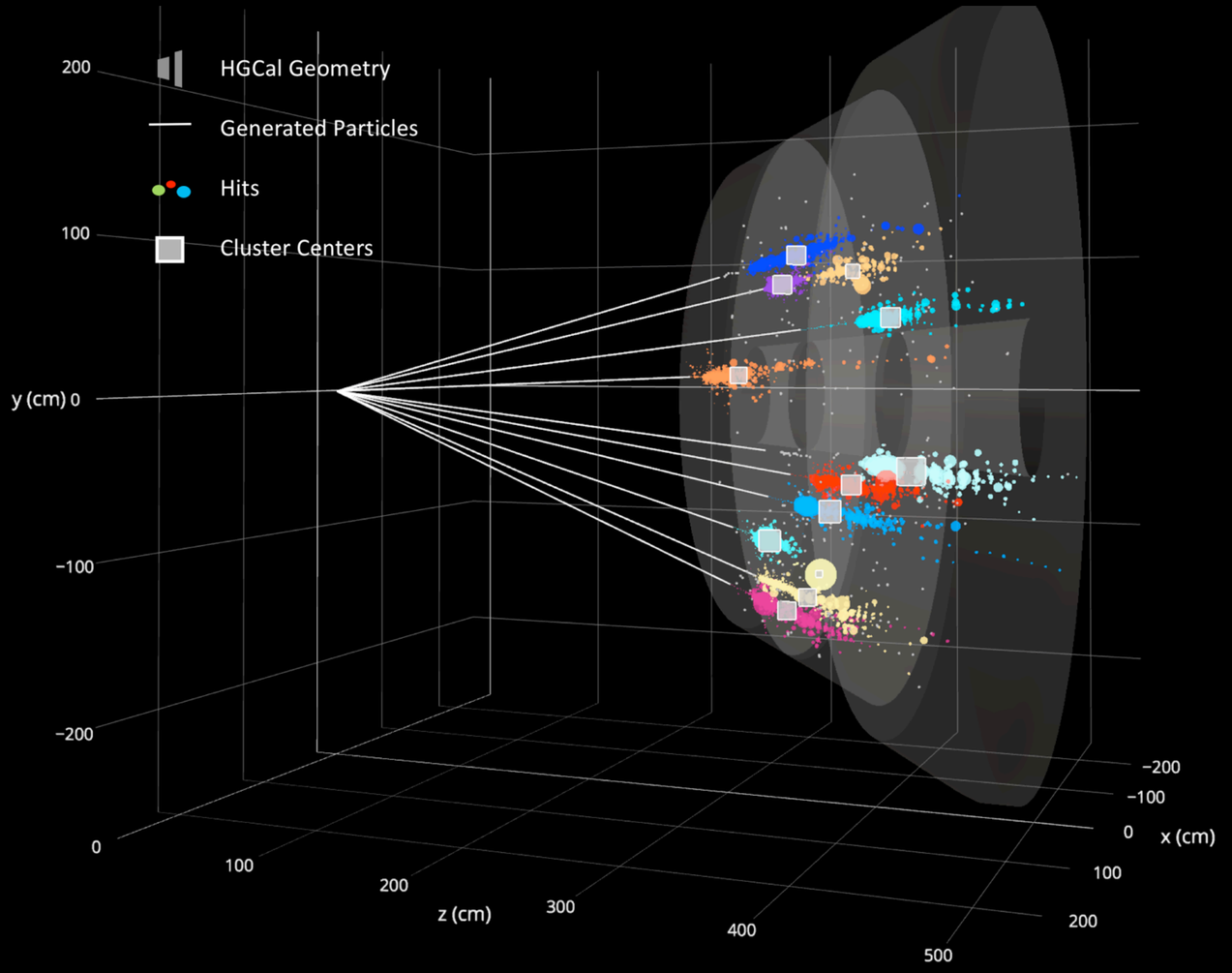

ML for HGCAL

Calculate features of edges and designate as signal or noise

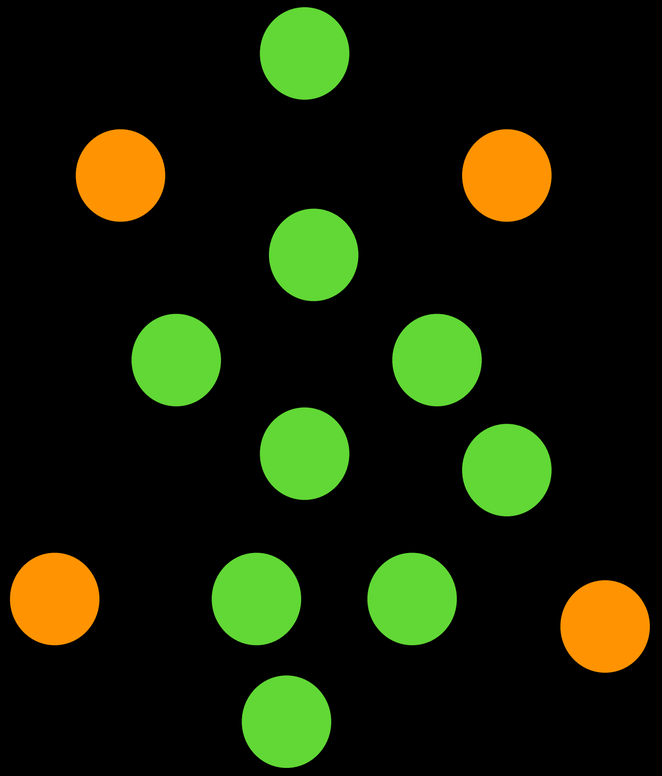

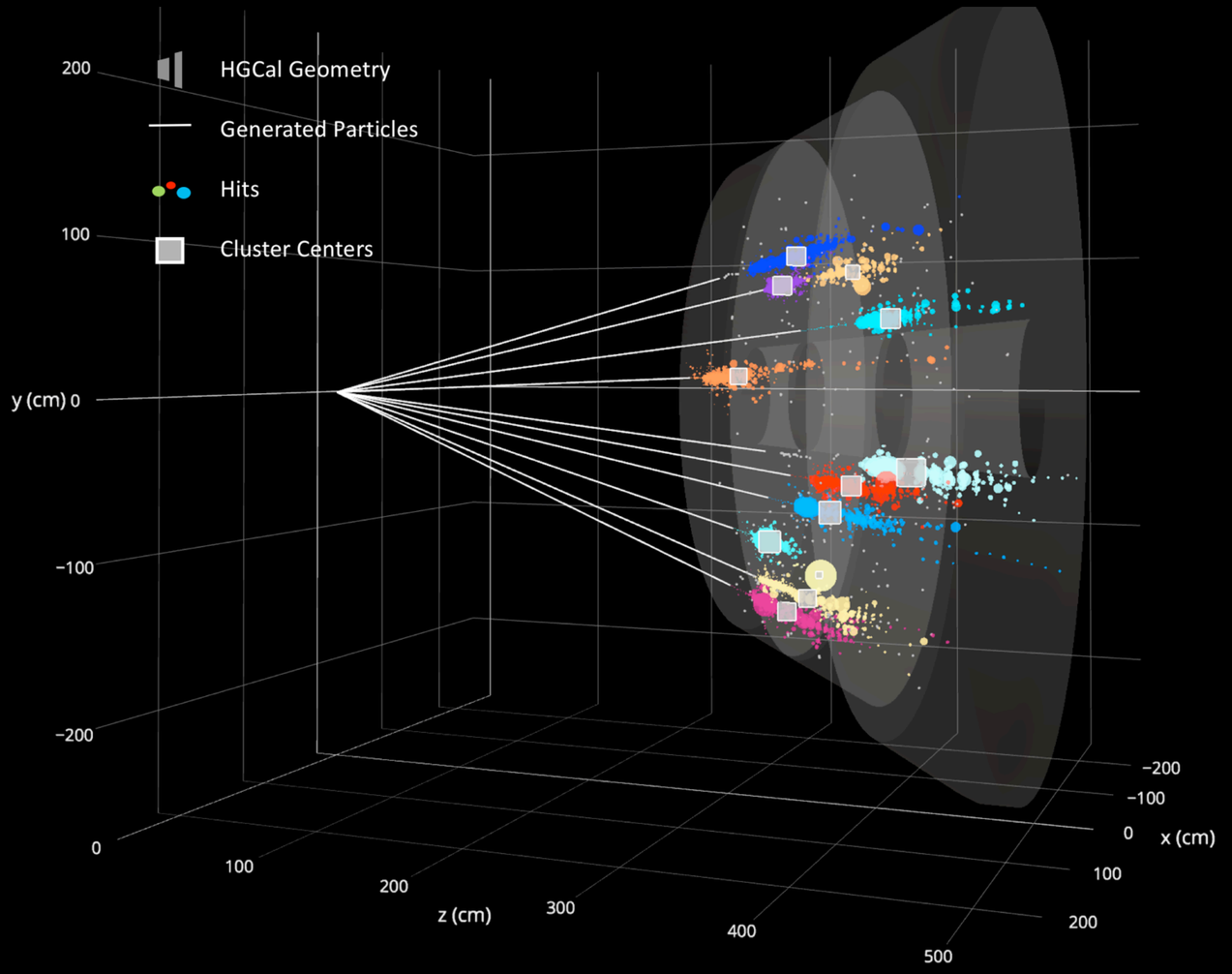

ML for HGCAL

Calculate features of edges and designate as signal or noise

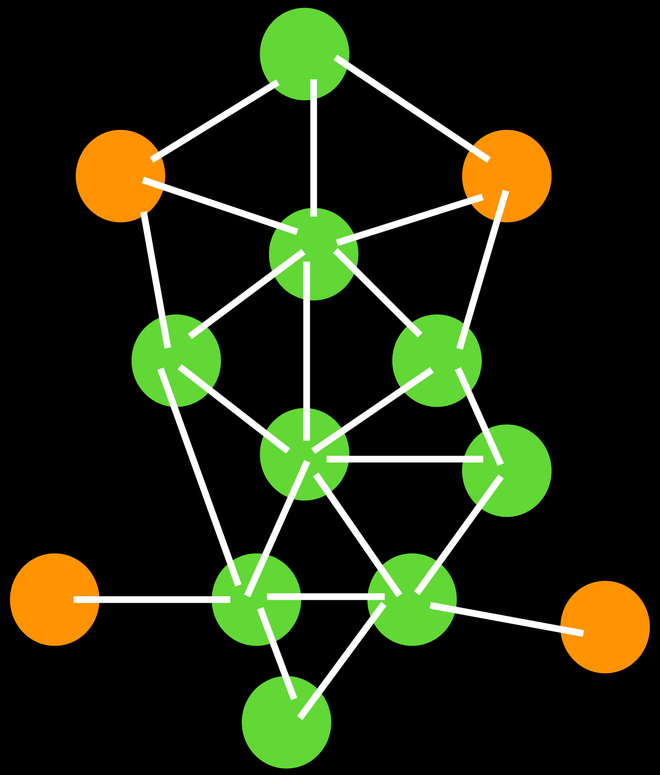

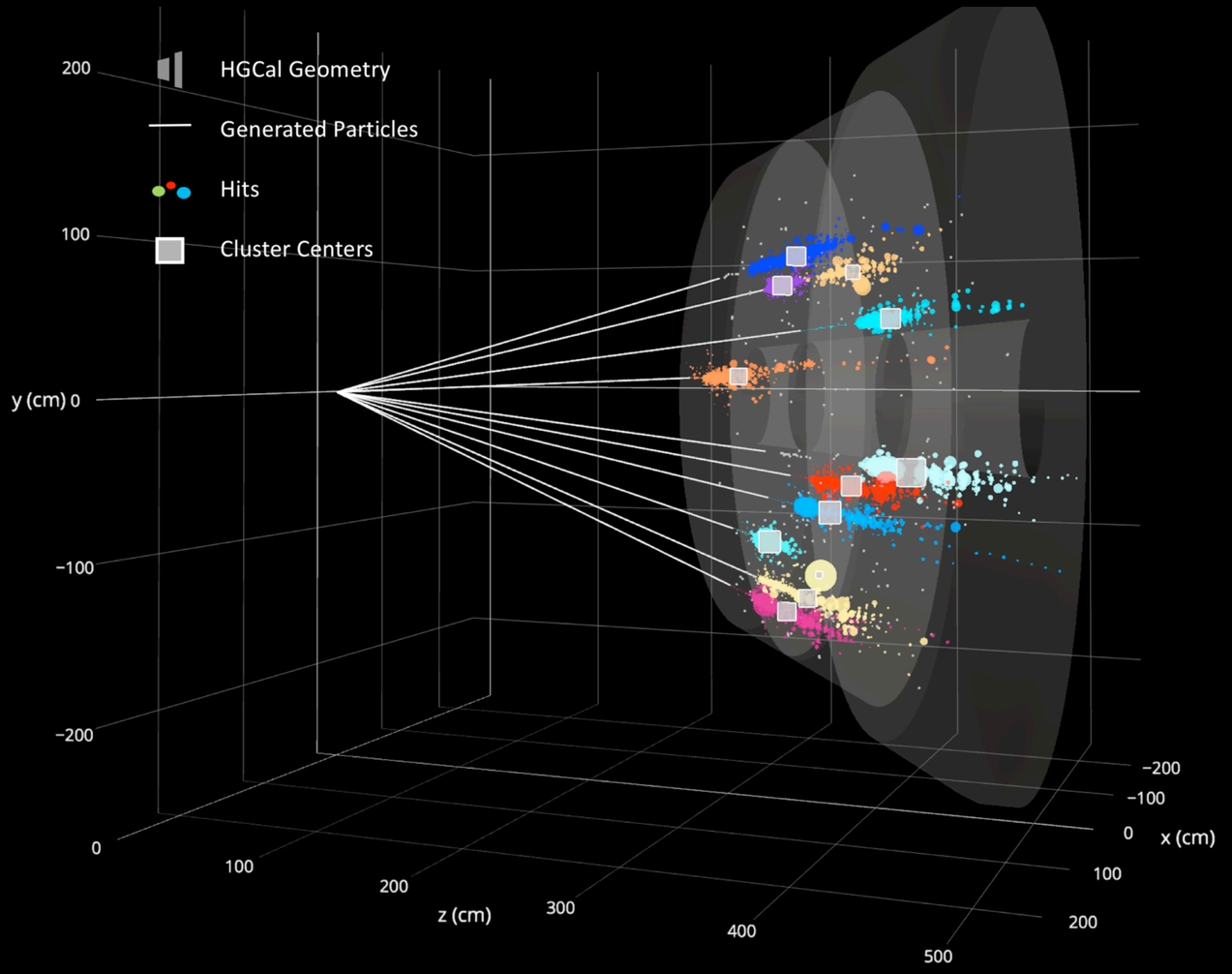

Distinguishing particle showers from hadronic taus (τ)

CMS *Simulation Preliminary*

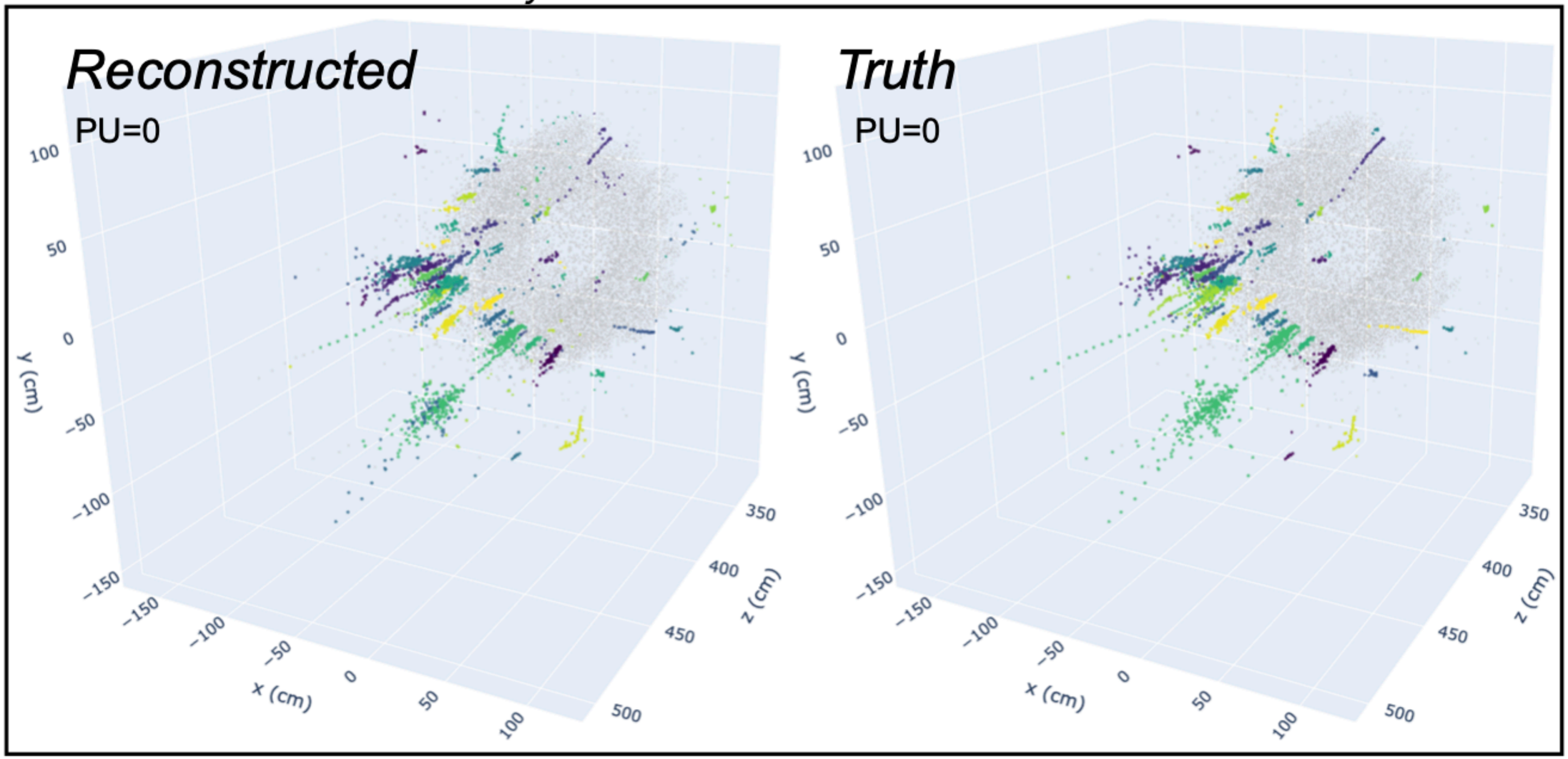

Using Graph Neural Networks (GNN) for HGCAL reconstruction

- The version of the HGCAL used in this talk
  - Implementation of geometry in `CMSSW_11_3_0_pre3`
  - This is done to use the trainings performed with di-τ events and extend them to single particle performance

Active Elements:
- Hexagonal modules based on Si sensors in CE-E and high-radiation regions of CE-H
- "Cassettes": multiple modules mounted on cooling plates with electronics and absorbers
- Scintillating tiles with on-tile SiPM readout in low-radiation regions of CE-H

Key Parameters:
Coverage: $1.5 < |\eta| < 3.0$
~215 tonnes per endcap
Full system maintained at -35°C
~620m^2 Si sensors in ~30000 modules
~6M Si channels, 0.5 or 1cm^2 cell size
~400m^2 of scintillators in ~4000 boards
~240k scint. channels, 4-30cm^2 cell size
Power at end of HL-LHC:
~125 kW per endcap

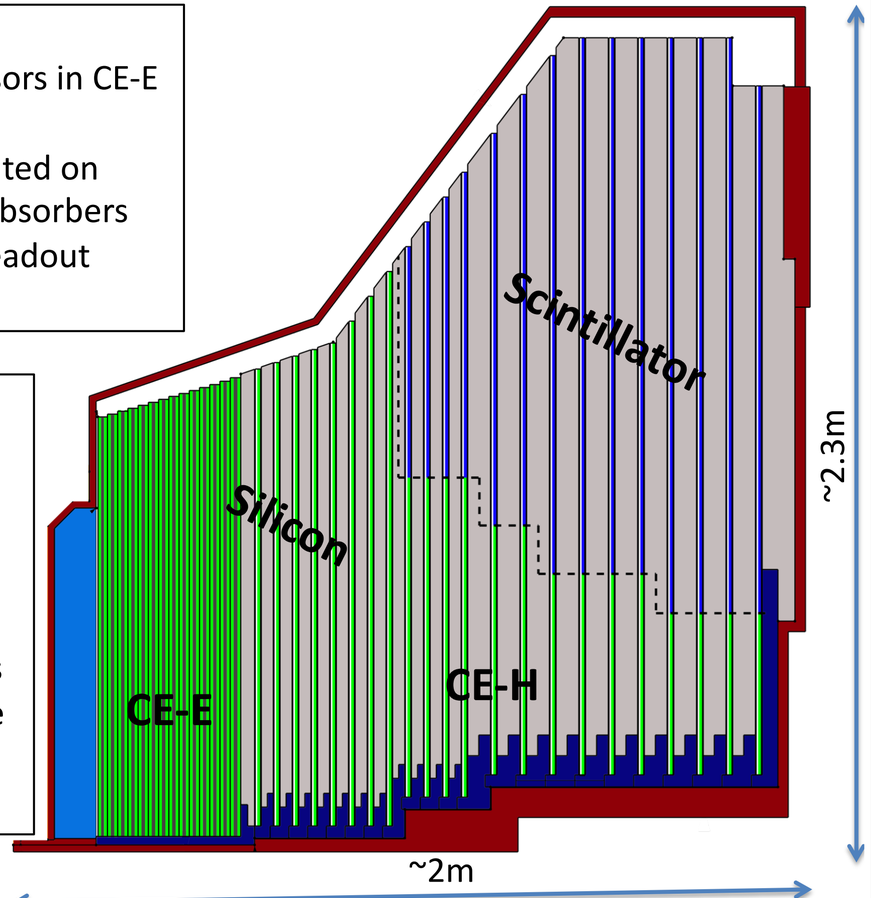

Electromagnetic calorimeter (**CE-E**): **Si**, Cu & CuW & Pb absorbers, 28 layers, 25 X_0 & ~1.3λ
Hadronic calorimeter (**CE-H**): **Si** & **scintillator**, steel absorbers, 22 layers, ~8.5λ

The network

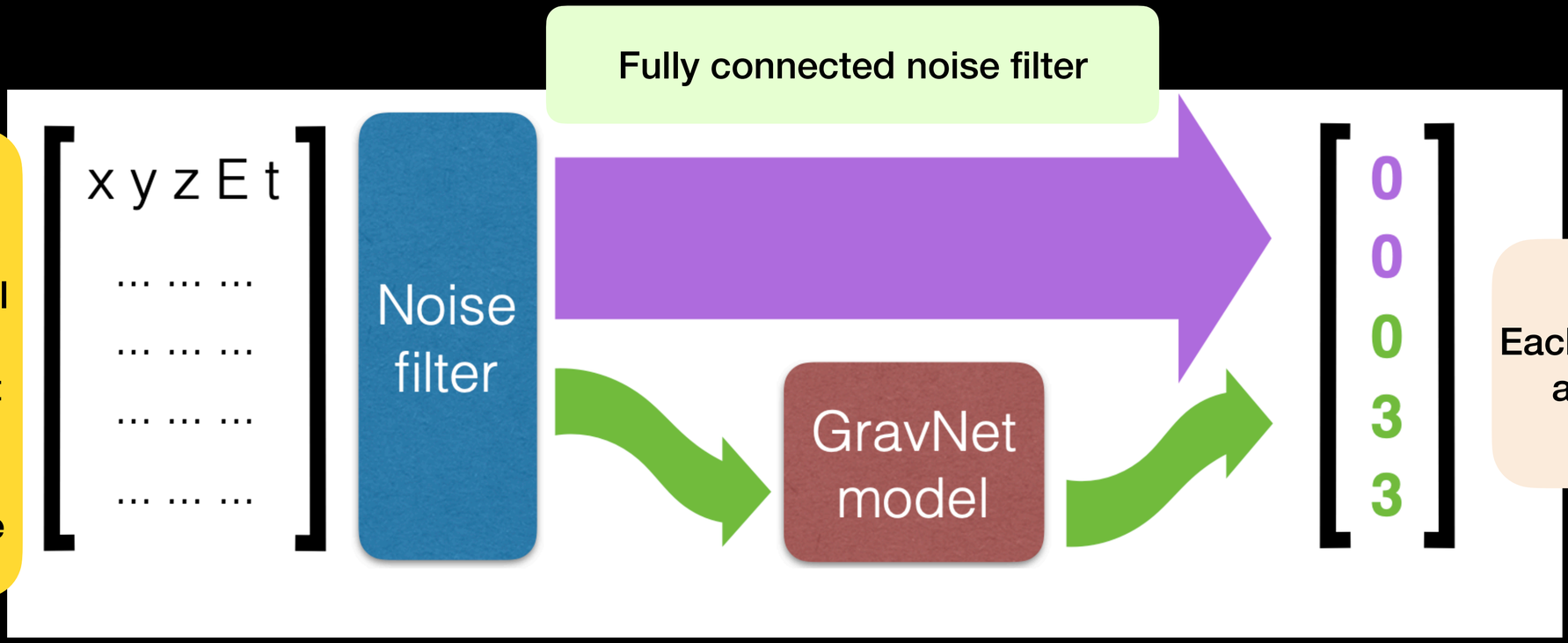

Hit-level quantities GEANT4 with modified truth level information→ additional incident particle history All hits given as input (95% hits are noisy)

Each hit is assigned a cluster label

- "GravNet" message passing convolutional operator (https://arxiv.org/pdf/2106.01832)
  - Distance weighted dynamic GNN
    - Build representation of each vertex in the graph by aggregating information from 64 nearest neighbors
- Trained with "Object Condensation" loss function (Eur. Phys. J. C 80, 886 (2020))

The definition of loss

- The loss function is based on the concept of attractive and repulsive potentials
  - Charge defined per vertex
    - Zero gradient at 0 and monotonically increasing at 1
  - Vertices belonging to the same object are pulled towards the condensation point with highest charge (attractive)
  - Vertices not belonging to the object are pushed away (repulsive)

Extending the di-τ training to single particles

- ☑ Results with the τ-dataset performant
- ☑ Demonstrating that trainings are robust across various particle types: many→one correspondence holds
- ☑ Use the *same* training on a single particle dataset
- ☑ Generated the single photon (PDG ID: 22), charged pion ($\pi^{\pm}$, PDG ID: 211) and K_L^0 (PDG ID: 130) sample with a `CloseByParticleGunProducer`
  - ☑ `CMSSW_11_3_0_pre3`
  - ☑ Set energy to [2, 3, 5, 10, 25, 50, 75, 100, 200, 300, 500, 1000] GeV
  - ☑ Used cms-pepr and production_tests
  - ☑ Changed `FlatEtaRangeGunProducer` to `CloseByParticleGunProducer` with an appropriate change of parameters
    - ☑ `CloseByParticleGunProducer` includes some additional parameters and set these parameters to values recommend by the DPG on the HGCAL website

Performance of the trained model on pion showers

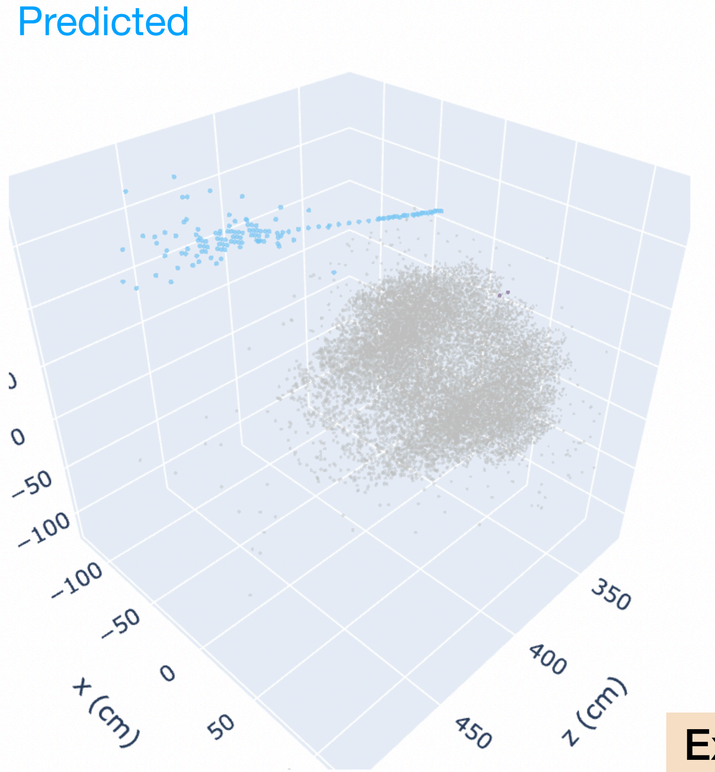

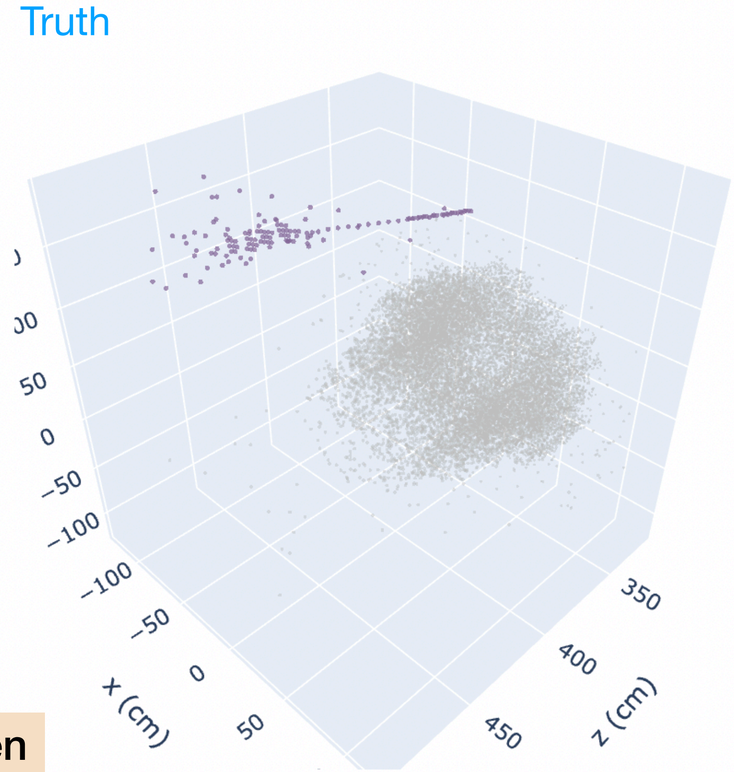

Excellent performance when using trained model to ascertain single particle response

The suppression of noise

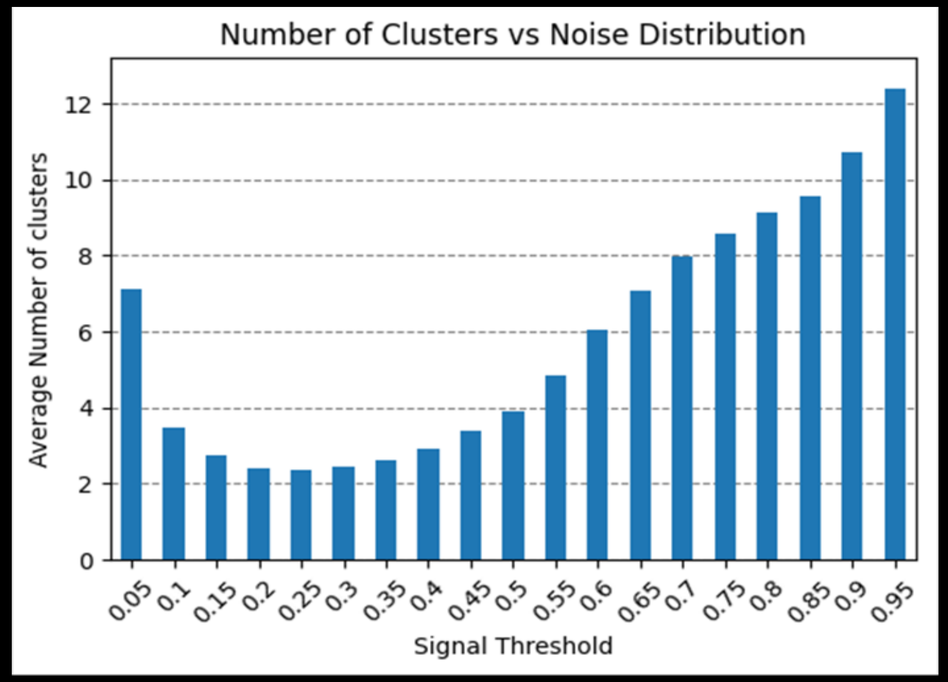

Photons

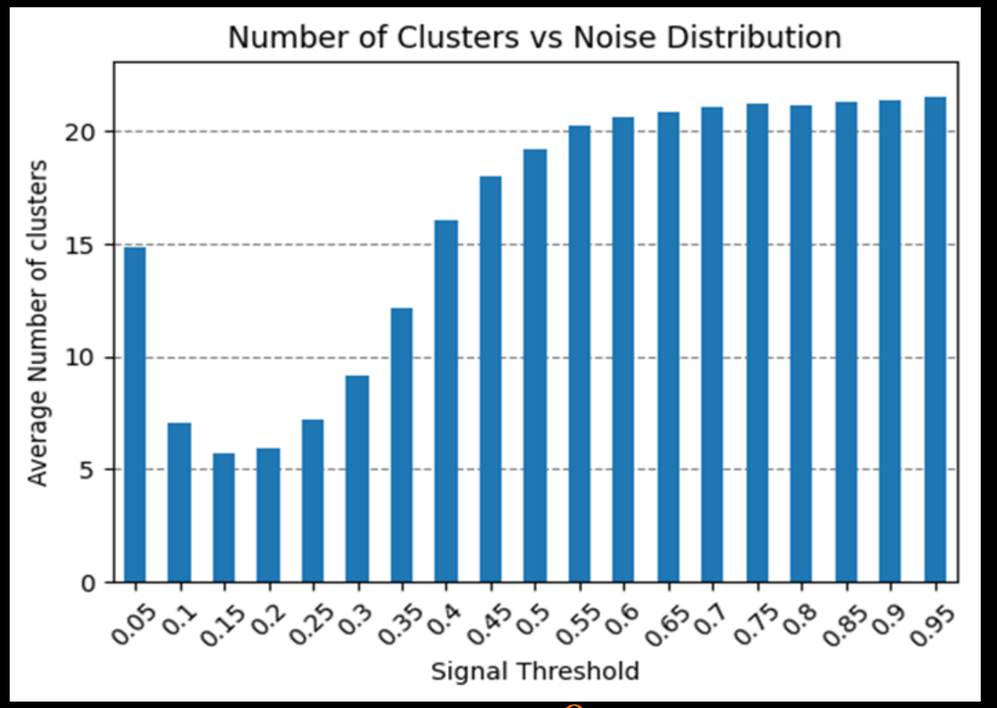

K_L^0

Energy resolution — Photons

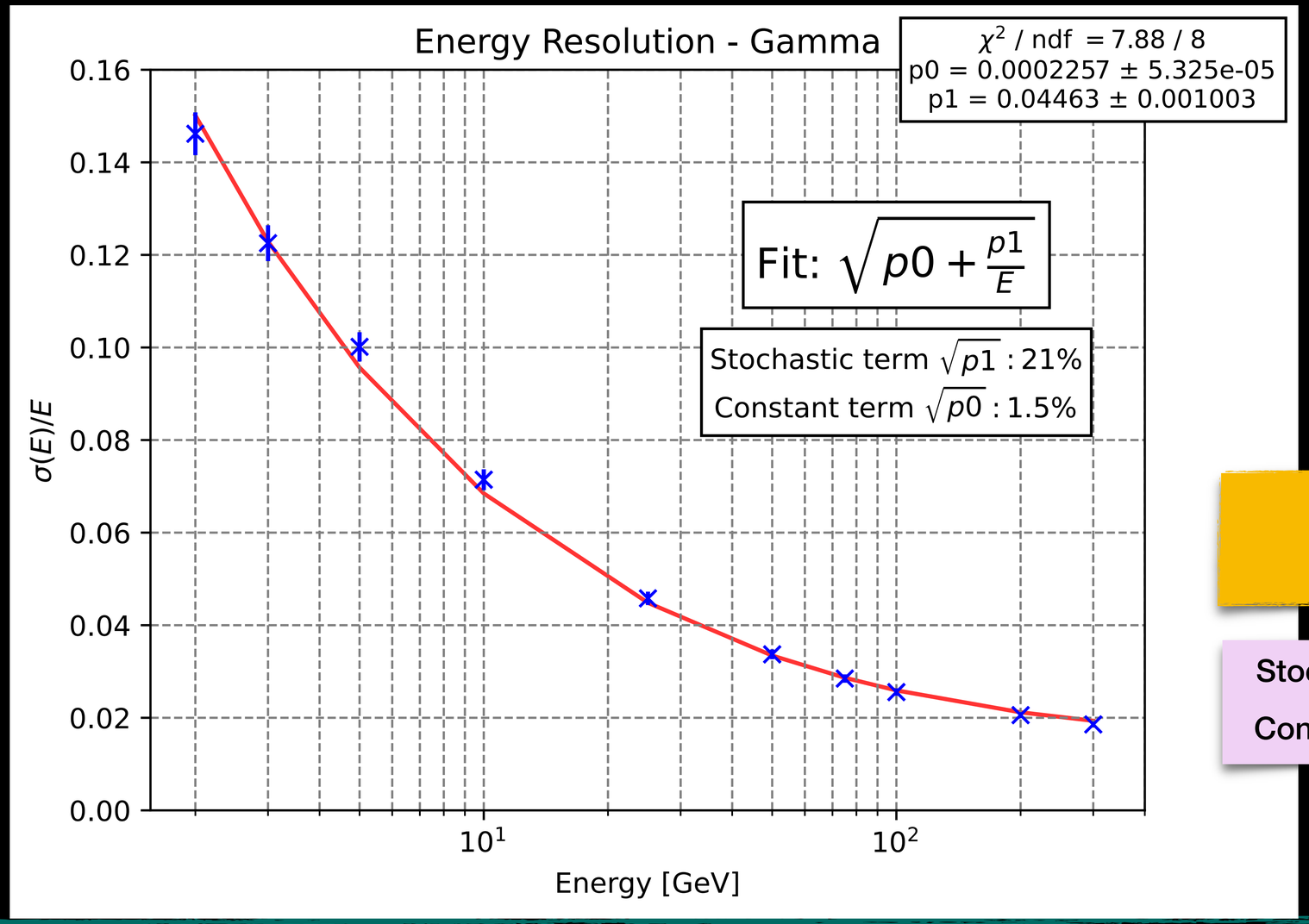

Excellent efficiency of reconstructing low energy clusters

Fit: $\sqrt{p_0 + \frac{p_1}{E}}$

Stochastic term $\sqrt{p_1}$: 21 %

Constant term $\sqrt{p_0}$: 1.5 %

Energy resolution – K_L^0

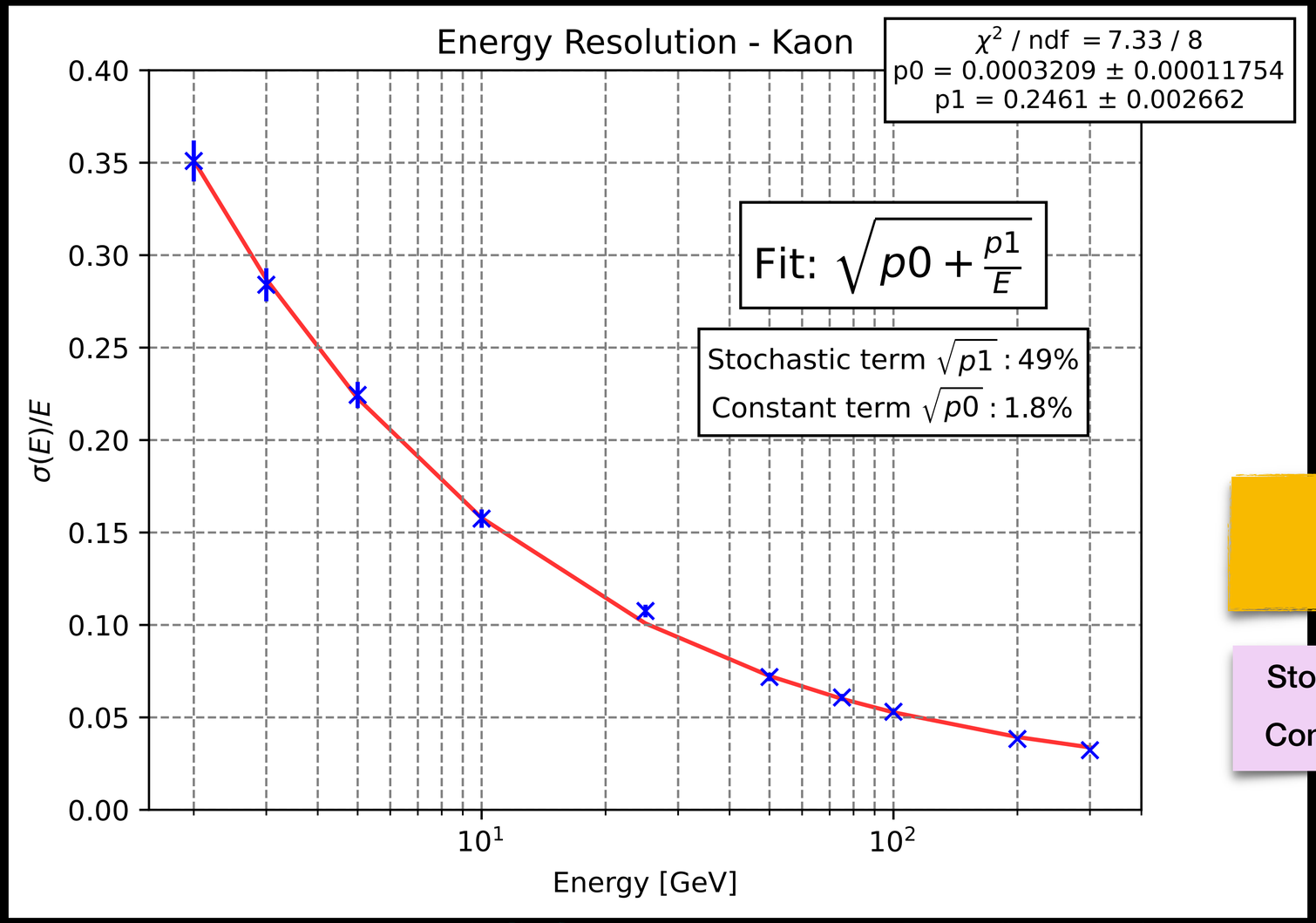

Excellent efficiency of reconstructing low energy clusters

Fit: $\sqrt{p_0 + \frac{p_1}{E}}$

Stochastic term $\sqrt{p_1}$: 49 %

Constant term $\sqrt{p_0}$: 1.8 %

Energy resolution — $\pi^{\pm}$

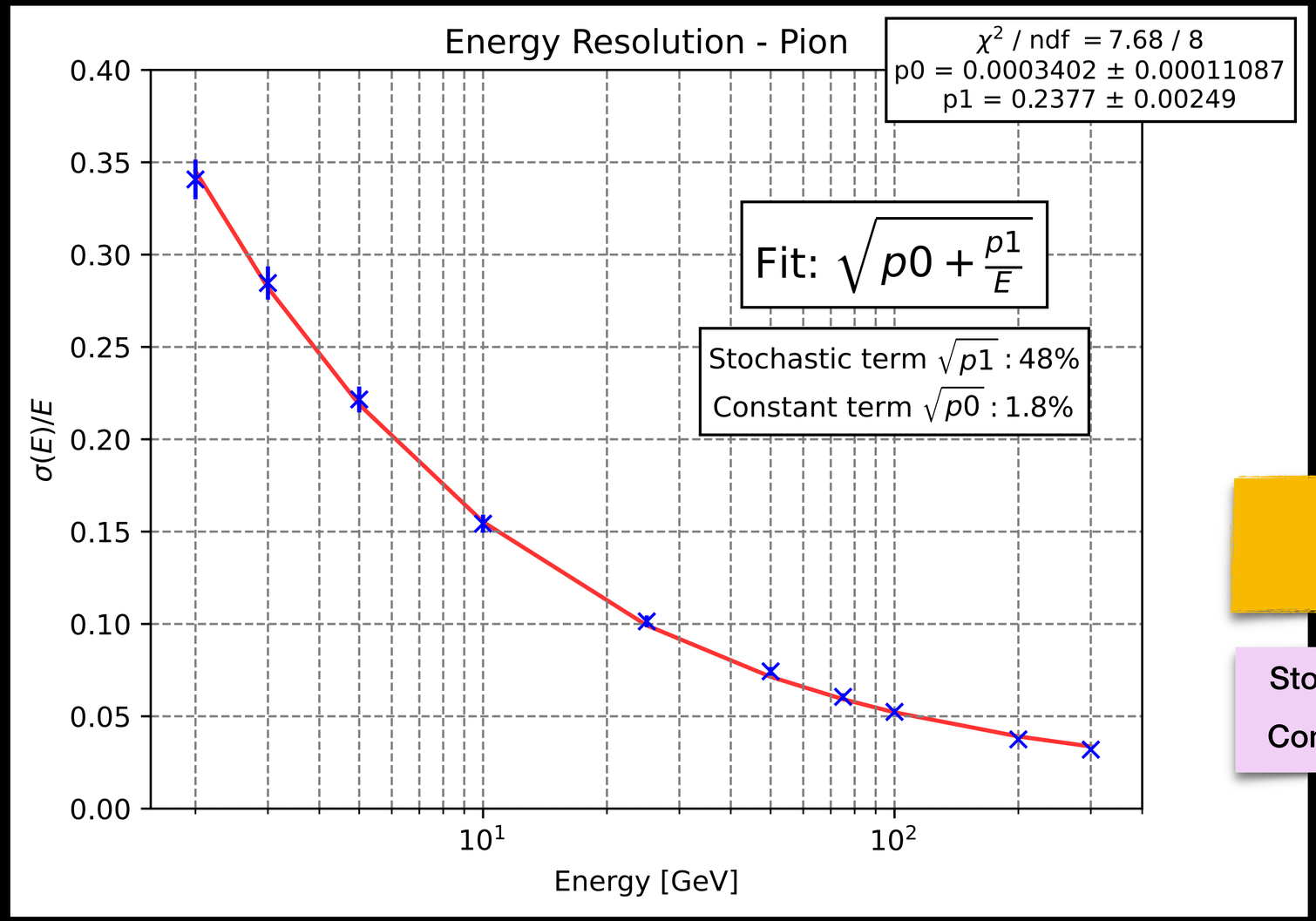

Excellent efficiency of reconstructing low energy clusters

Fit: $\sqrt{p_0 + \frac{p_1}{E}}$

Stochastic term $\sqrt{p_1}$**: 48 %**

Constant term $\sqrt{p_0}$**: 1.8 %**

Does it close? Yes!

- τ trainings on the τ dataset: τ dataset where incident particles are single taus (PDG ID: ±15)

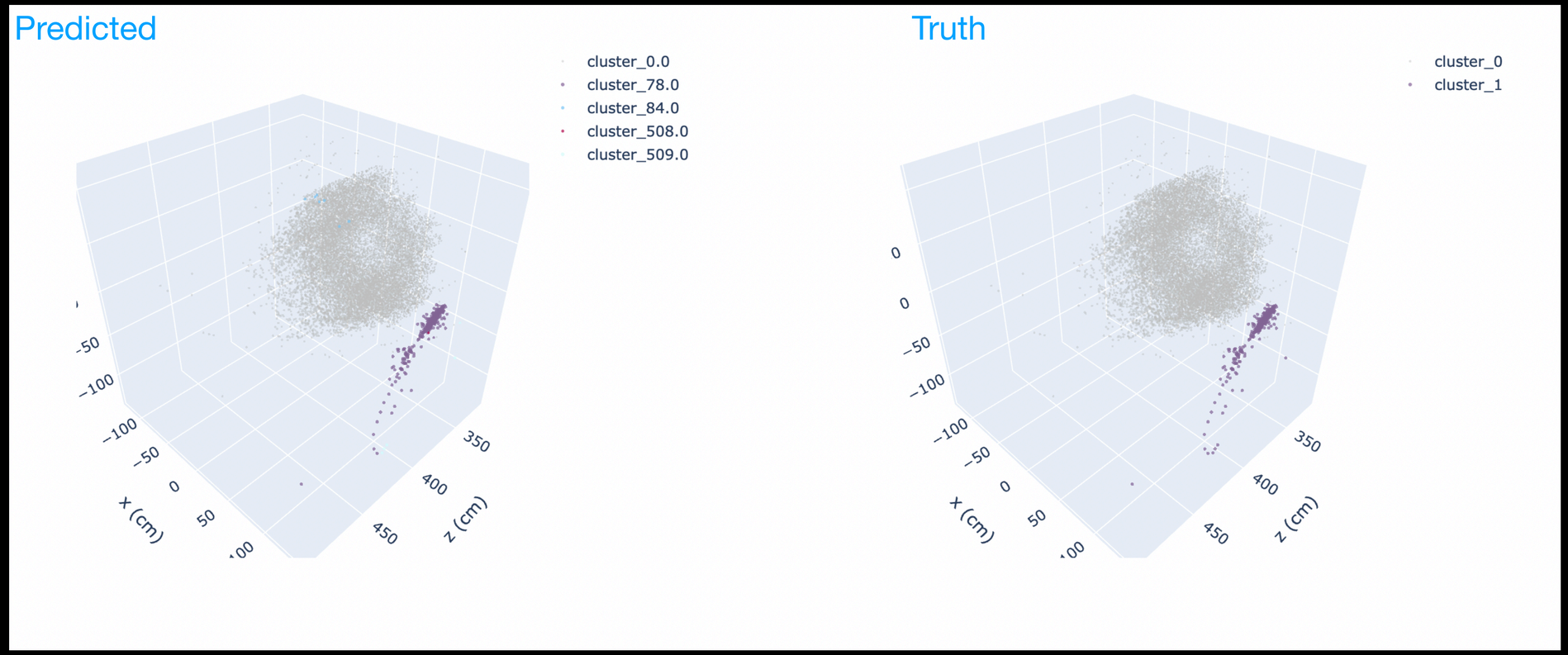

Tau performance: need to improve

Excellent efficiency of reconstructing low energy clusters

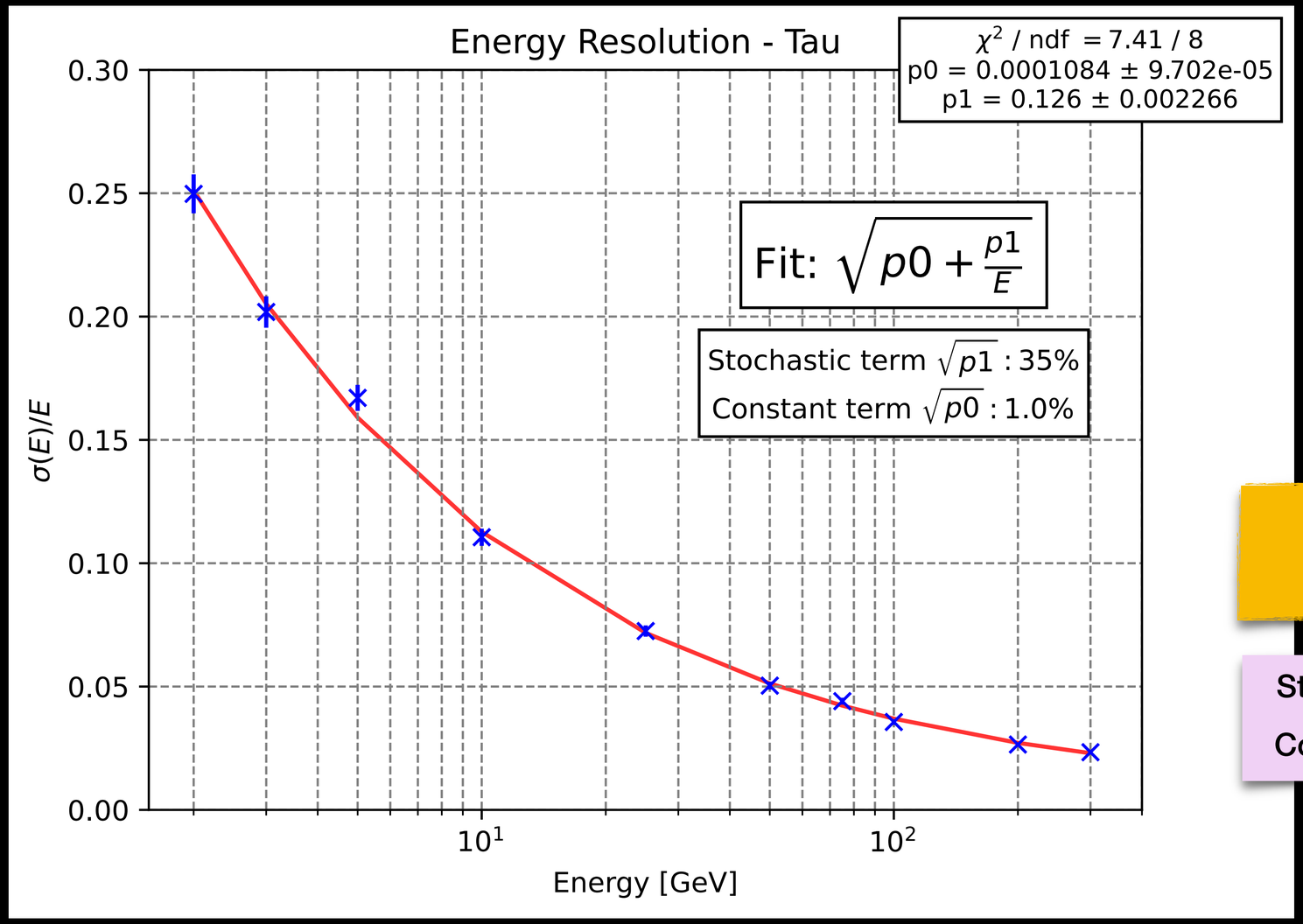

Fit: $\sqrt{p_0 + \frac{p_1}{E}}$

Stochastic term $\sqrt{p_1}$**: 35 %**

Constant term $\sqrt{p_0}$**: 1.0 %**

What's next?

- Update trainings with the newest HGCAL geometry
  - Extraction of position/timing resolution in progress with current training
- Extend training to higher energy ranges to get better coverage in the high energy region
  - Improve constant term
  - Stochastic term already low due to excellent performance of the algorithm in the low energy region